



HAL
open science

Oxidation-promoted synthesis of ferrocenyl planar chiral rhodium(iii) complexes for C–H functionalization catalysis

Julien Cabanes, Maksym Odnoroh, Carine Duhayon, Christian Bijani, Alix Sournia-Saquet, Rinaldo Poli, Agnès Labande

► To cite this version:

Julien Cabanes, Maksym Odnoroh, Carine Duhayon, Christian Bijani, Alix Sournia-Saquet, et al.. Oxidation-promoted synthesis of ferrocenyl planar chiral rhodium(iii) complexes for C–H functionalization catalysis. *Mendeleev Communications*, 2021, 31 (5), pp.620-623. 10.1016/j.mencom.2021.09.010 . hal-03412564

HAL Id: hal-03412564

<https://hal.science/hal-03412564v1>

Submitted on 3 Nov 2021

HAL is a multi-disciplinary open access archive for the deposit and dissemination of scientific research documents, whether they are published or not. The documents may come from teaching and research institutions in France or abroad, or from public or private research centers.

L'archive ouverte pluridisciplinaire **HAL**, est destinée au dépôt et à la diffusion de documents scientifiques de niveau recherche, publiés ou non, émanant des établissements d'enseignement et de recherche français ou étrangers, des laboratoires publics ou privés.

Oxidation-promoted synthesis of ferrocenyl planar chiral rhodium(III) complexes for C-H functionalization catalysis

Julien Cabanes,[†] Maksym Odnoroh,[†] Carine Duhayon,[†] Christian Bijani,[†] Alix Sournia-Saquet,[†] Rinaldo Poli^{†,‡} and Agnès Labande^{*,†}

[†] *LCC-CNRS, Université de Toulouse, CNRS, INPT, F-31077 Toulouse, France ; e-mail : agnes.labande@lcc-toulouse.fr*

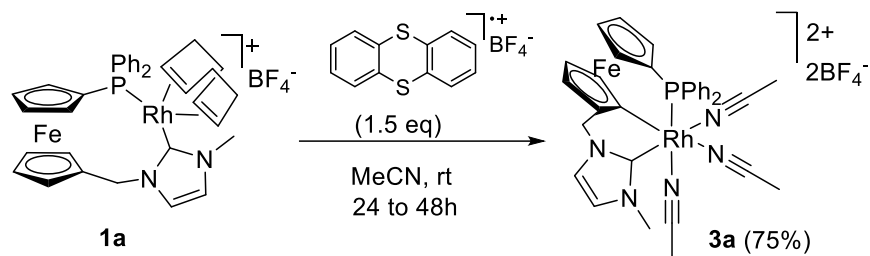
[‡] *Institut Universitaire de France, 1 rue Descartes, 75231 Paris, France.*

Abstract: The chemical oxidation of rhodium(I) complexes [Rh(L)(COD)][BF₄], where L is a ferrocenyl phosphine/*N*-heterocyclic carbene ligand, with 2 equivalents of a triarylammonium salt [N(4-BrC₆H₄)₃][BF₄] in acetonitrile gave planar chiral, air-stable [Rh(L)(MeCN)₃][BF₄]₂ complexes where the ferrocene (C₅H₄CH₂Im^R or C₅H₄CH₂BIm^{CH₂Mes}) ring has been C-H activated at the 2 position in good to excellent yields. An important reactivity difference between our complexes and the ubiquitous [Cp*^{*}Rh(MeCN)₃]₂X₂ complex has been observed in the Grignard-type arylation of 4-nitrobenzaldehyde.

Keywords: rhodium, *N*-heterocyclic carbenes, ferrocene, redox active ligands, catalysis

The rhodium-catalyzed functionalization of C(sp²)-H bonds has become intensely studied as an atom-economical reaction that allows to access elaborate compounds.¹⁻¹⁰ In this context, [Cp*^{*}RhCl₂]₂ and [Cp*^{*}Rh(MeCN)₃]₂X₂ have been privileged catalysts for this reaction and to our knowledge, there is only one example reporting *catalytic* C-H activation with a non-half-sandwich complex.¹¹ As three coordination sites are required for the reaction to proceed, it is very difficult to design new ligands that allow improving activities and selectivities, and developing asymmetric versions.¹²⁻²⁰ In this context, new rhodium(III) complexes bearing planar chiral ferrocenyl *N*-heterocyclic carbene (NHC)/phosphine ligands were obtained by oxidation of the corresponding rhodium(I) complexes, followed by activation of a ferrocene C-H bond. In this work, an optimized synthesis of the original complex^{21,22} (Scheme 1) is described, and various imidazolylidene substituents are introduced on the NHC moiety in order to study the stereoelectronic effects on the catalytic activity in the Grignard-type arylation of 4-nitrobenzaldehyde. The synthesis of rhodium(III) complex **3a** was previously carried out starting either from rhodium(I) complex **1a**, bearing a COD ligand,²¹ or from the corresponding dicarbonyl rhodium(I) complex.²² Both methods have their disadvantages: the reaction was easily performed using the mild oxidant AgBF₄ from the dicarbonyl complex, but the latter is

moderately bench-stable and has to be prepared from **1a**; on the other hand, a stronger and moderately stable oxidant, thianthrenium tetrafluoroborate [Th]⁺[BF₄⁻], was necessary to drive the reaction to completion with complex **1a**, which bears the more strongly coordinated COD ligand (Scheme 1).

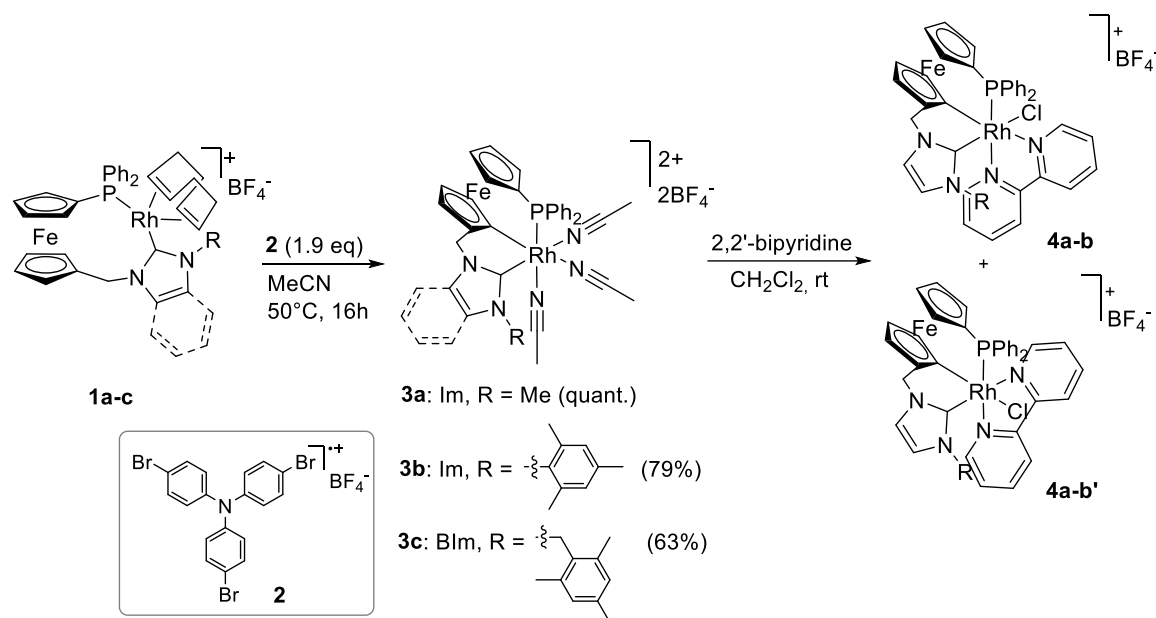


Scheme 1. Previous synthesis of rhodium(III) complex **3a**.

We therefore focused our efforts on finding new efficient yet stable oxidants to optimize the synthesis of **3a** directly from **1a** and opted for the triarylammonium salt [N(4-BrC₆H₄)₃]⁺[BF₄⁻] **2** (Scheme 2).²³ The latter is a weaker oxidant compared to [Th]⁺[BF₄⁻] ($E^{\circ}_{1/2} = 0.67$ V and 0.86 V vs. [FcH/FcH⁺] in MeCN, respectively), but more stable and therefore easier to handle and store. The reaction of complex **1a** with 1.9 equivalents of **2** went smoothly at 50°C, the driving force being the precipitation of N(4-BrC₆H₄)₃ in acetonitrile. Complex **3a** was easily retrieved in quantitative yield (Scheme 2). With the aim of studying the influence of the stereoelectronic properties on the catalytic activity, we applied the new synthetic conditions to other rhodium(I) complexes.^{24, 25} Thus **1b** was chosen for its bulky mesityl substituent on the imidazol-2-ylidene (Im) moiety, whereas **1c** possesses a more flexible CH₂-mesityl substituent on the nitrogen atom but a bulkier and slightly less donating benzimidazol-2-ylidene (BIm) unit. The expected rhodium(III) complexes **3b** and **3c** were obtained as deep red, air-stable solids in 79% and 63% yield, respectively (Scheme 2).

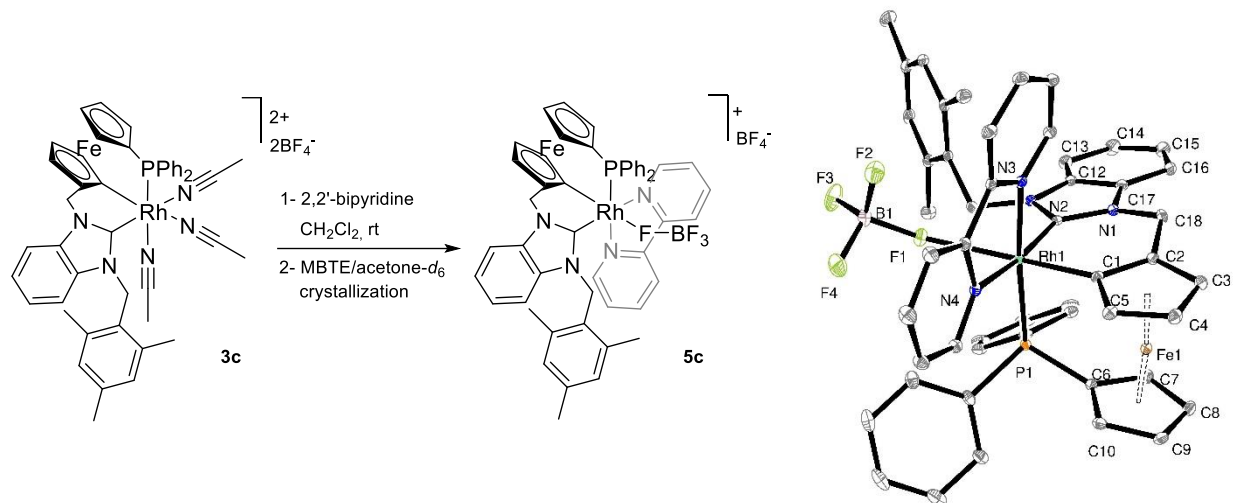
All rhodium(III) complexes were characterized by multinuclear NMR and HR-MS (see S.I.). The NMR data unambiguously shows the C-H activation of the ferrocene C-H bond: only seven proton resonances for the ferrocenyl unit are present in the ¹H NMR spectra, as well as three resonances for quaternary carbons in the ferrocene region of the ¹³C NMR spectra. A characteristic signal was observed for the carbenic carbon as a doublet of doublets at 147.6 ppm for **3b**, and at 161.4 ppm (app. doublet of doublets) for **3c**. These

values are in the range of those expected for similar rhodium(III) complexes (e.g. complex **3a**).^{21, 26, 27} Finally, the ³¹P analysis shows a doublet at 41.2 ppm for **3b** and 40.9 ppm for **3c**, typical of a phosphorus linked to a rhodium(III) center.



Scheme 2. Optimized synthesis of rhodium(III) complexes **3a-c** and derivatization of **3a-b**.

Since complexes **3b** and **3c** could not be crystallized, they were reacted with 1.5 equivalents of 2,2'-bipyridine (bipy) in CH₂Cl₂ to yield orange-red solids (Scheme 2), the ¹H and ¹³C NMR spectra of which were too complex for a structural analysis. The ³¹P NMR spectrum of **4b** in acetone-*d*₆ displays only two doublets at 32.2 ppm (*J*_{RhP}=120.5 Hz) and 29.9 ppm (*J*_{RhP}=124.5 Hz) in a 1:1 ratio, similar to what was observed with **4a**.²¹ This may indicate the formation of the expected compounds, with the bipy and one chloride occupying the three acetonitrile positions, as a mixture of diastereomers (**4b+4b'**). The ³¹P NMR spectrum of **3c** + bipy shows a more complex behavior: three doublets, of varying intensity according to the reaction batch, are observed in the same region on the ³¹P NMR spectrum, at 36.3 ppm (*J*_{RhP}=119.6 Hz), 35.8 ppm (*J*_{RhP}=129.7 Hz) and 32.8 ppm (*J*_{RhP}=123.6 Hz). Several species were probably present.



Scheme 3. Derivatization of complex **3c** and ORTEP view of compound **5c**. Ellipsoids are shown at the 30% probability level. All hydrogens are omitted for clarity.

Selected bonds (Å) and angles (°) : Rh(1)-P(1) = 2.3711(3), Rh(1)-C(1) = 1.9912(12), Rh(1)-C(11) = 2.0330(12), Rh(1)-N(3) = 2.0808(10), Rh(1)-N(4) = 2.1291(10), Rh(1)-F(1) = 2.3500(7), B(1)-F(1) = 1.4512(17); P(1)-Rh(1)-C(1) = 90.06(3), P(1)-Rh(1)-C(11) = 85.92(3), C(1)-Rh(1)-C(11) = 91.62(5), P(1)-Rh(1)-N(3) = 174.70(3), C(1)-Rh(1)-N(3) = 84.73(4), C(11)-Rh(1)-N(3) = 93.26(4), P(1)-Rh(1)-N(4) = 102.67(3), C(1)-Rh(1)-N(4) = 88.90(4), C(11)-Rh(1)-N(4) = 171.40(4), N(3)-Rh(1)-N(4) = 78.23(4), P(1)-Rh(1)-F(1) = 98.50(2), C(1)-Rh(1)-F(1) = 165.42(4), C(11)-Rh(1)-F(1) = 100.71(4), N(3)-Rh(1)-F(1) = 86.80(3), N(4)-Rh(1)-F(1) = 77.75(3).

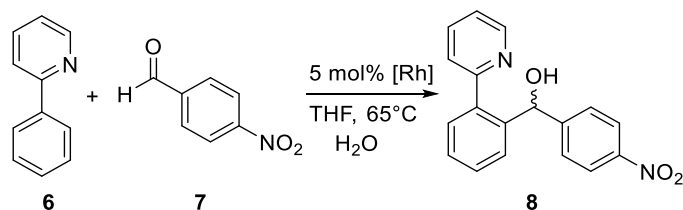
Pleasingly, careful layering of methyl *tert*-butyl ether (MTBE) on a solution of **3c** in acetone-*d*₆ gave deep red X-ray quality crystals of **5c** (Scheme 3). The crystal structure confirmed the presence of a σ bond between the NHC-functionalized Cp ring and the rhodium center. As in the case of [Rh(L)Cl(bipy)][BF₄] **4a**, one bipy occupies two of the three MeCN coordination positions in **5c**. However, instead of a chloride abstracted from the solvent as in the case of **4a**, the last position in **5c** was surprisingly occupied by a κ^1 :F-coordinated BF₄ ligand. Crystal structures containing Rh-FBF₃ bonds are quite unusual and only five other

examples with rhodium(III) have been reported so far by Milstein²⁸⁻³¹ and Breit.³² The BF₄⁻ anion is coordinated *trans* to the Rh-C bond at ferrocene, with a Rh(1)-F(1) distance of 2.3500(7) Å, which is in the range of previously reported Rh-F bond distances. This structure confirms the presence of the Rh-C bond at ferrocene with a *fac* arrangement of the tridentate ligand. The bipy ligand is situated *trans* to the NHC and phosphine ligands. All other distances are within the expected range for this type of complex, and most are similar to those observed for **4a**, with the noticeable exception of Rh(1)-P(1) distance, which is longer in **5c**: this may account for the high strain exerted on the ligand to keep the tridentate coordination: the latter adopts a severely distorted geometry to accommodate the octahedral coordination of rhodium. Indeed, the metal coordination forces the phosphorus atom to deviate significantly from the plane of the Cp ring to which it is attached by 0.350(1) Å, and tilts the two ferrocene cyclopentadienyl units to a dihedral angle of 10.01(5)°. In the same way as for **4a**, both planar chirality at ferrocene *and* central chirality at the metal are now present, hence the potential production of up to three diastereoisomers (given the imposed *fac* stereochemistry of the tridentate ligand). However, in the present case a different diastereoisomer crystallized (the bipy ligand was situated *trans* to the phosphine and to the Rh-C bond at ferrocene in the case of **4a**). For the latter, DFT calculations carried out on the three possible isomers had shown that the calculated electronic energies of two isomers were relatively close (ΔG of 3.7 kcal.mol⁻¹), whereas the third one – with the bipy ligand *trans* to the NHC ligand and the Rh-C bond at ferrocene, not observed experimentally – had a much higher energy minimum (8.4 kcal.mol⁻¹ relative to the most stable isomer), which was explained by severe steric constraints.²¹ The same limitations seem to apply here.

Complexes **3a-c** were then evaluated as catalysts in the Grignard-type arylation of 4-nitrobenzaldehyde with 2-phenylpyridine. (table 1).³³ Indeed, Rh^{III} complexes bearing three coordination sites available for C(sp²)-H functionalization catalysis are very often restrained to Cp-based architectures,⁷⁻⁹ and our system seemed interesting in that regard. The reaction worked well with anhydrous THF but an optimum was found with 1.5 equivalents of H₂O relative to 2-phenylpyridine (51% conversion, entry 3). Average conversions were obtained after 24 h and increasing the reaction time did not allow to improve significantly the conversion

(58% after 48 h, entry 4). Unfortunately, complexes **3b** and **3c** gave none of the expected product and only starting materials were detected (entries 7 and 8). In order to check whether the steric limitations could be responsible for this lack of reactivity, a bulkier substrate – 1-(2-methylphenyl)-isoquinoline – was used instead of 2-phenylpyridine (entry 9). Again, no trace of the expected product was observed.

Table 1. Grignard-type arylation of 4-nitrobenzaldehyde



Entry	[Rh]	H ₂ O (equiv. vs. 6)	Conversion (%) ^b
1	3a	-	43
2	3a	1	50
3	3a	1.5	51
4 ^c	3a	1.5	58
5	3a	3	36
6	3a	10	33
7	3b	1.5	n.r.
8	3c	1.5	n.r.
9 ^d	3a	1.5	n.r.
10	1a	1.5	n.r.
11	1b	1.5	n.r.
12	1c	1.5	n.r.

^a Conditions: 2-phenylpyridine (1.0 equiv.), 4-nitrobenzaldehyde (2.0 equiv.), [Rh] (5 mol%), H₂O (x equiv.), THF (0.5 mL, 0.4M), 65°C, 24h. ^b Calculated by integration of characteristic ¹H NMR signals of **6** and **8**. ^c Reaction time 48h. ^d 1-(2-methylphenyl)-isoquinoline used instead of 2-phenylpyridine.

In recent years, it has been shown that M-NHC bonds, although very strong, could cleave under chosen catalytic conditions and lead to active metallic species without NHC stabilizing ligand.³⁴ Whereas the cleavage of the Rh-NHC bond in **3a-c** seems unlikely, due to the tridentate nature of the ligand that stabilizes the structure, Rh^I precursors **1a-c** may behave differently. However, the latter proved completely inactive for this reaction under identical conditions: after 24h at 65°C, no trace of the expected product was observed and only starting materials were observed by ¹H NMR (table 1, entries 10-12). ³¹P NMR analysis of the crude mixture confirmed the integrity of the structure in **1a**, as the typical doublet at ca. 20 ppm was observed. Only traces of unidentified by-products were characterized by singlets at ca. 23 ppm and 39 ppm, and can explain the slightly brown aspect of the catalyst after reaction. This confirms the very high stability of rhodium(I) complexes **1a-c** under several reaction conditions,^{25,35} and the efficiency of the redox strategy described earlier to promote COD departure in the presence of MeCN. As in rhodium(III) complexes **3a-c**, the bidentate nature of the ligand, bearing strongly coordinating phosphine and NHC ligands, does not seem to favor the cleavage of the Rh-NHC bond.

Unfortunately, complexes **3a-c** also proved inactive as catalysts for the synthesis of 3,4-dihydroisoquinolones, whatever the conditions used.^{12, 13, 36} These results are rather surprising since our rhodium(III) complexes easily lose an acetonitrile ligand and either react with dichloromethane to coordinate a chloride (**3a**)²¹ or a BF₄⁻ anion (**3c**). It seems that the tridentate (NHC,P,C) ligands may be too sterically crowded and may prevent the approach of bulkier substrates, contrary to the ubiquitous [Cp**Rh*(MeCN)₃]²⁺ complex.³³

In conclusion, the synthesis of several planar chiral rhodium(III) complexes has been carried out by oxidation of rhodium(I) complexes containing an electroactive ferrocenyl unit. Optimized conditions have been developed with the use of a relatively mild, stable oxidant. Although the least sterically crowded complex allows the functionalization of 2-phenylpyridine with 4-nitrobenzaldehyde, no reaction occurred with complexes bearing bulkier ligands, pointing to an important reactivity difference between our complexes and the ubiquitous [Cp**RhCl*]₂ and [Cp**Rh*(MeCN)₃]*X*₂ complexes. Mechanistic studies are in progress to better understand the reasons of this low reactivity in C-H functionalization reactions.

Supporting Information

Synthetic procedures for all new compounds and for C-H functionalization reactions; cyclic voltammograms of complexes **1b** and **1c**; NMR spectra of complexes **3a-c** and of the products obtained from the reactions of **3b** and **3c** with bipy; X-ray data collection and structure determination of complex **5c**.

CCDC 1848989 contain the supplementary crystallographic data for this paper. These data can be obtained free of charge via www.ccdc.cam.ac.uk/data_request/cif, or by emailing data_request@ccdc.cam.ac.uk, or by contacting The Cambridge Crystallographic Data Centre, 12 Union Road, Cambridge CB2 1EZ, UK; fax: +44 1223 336033.

Acknowledgements

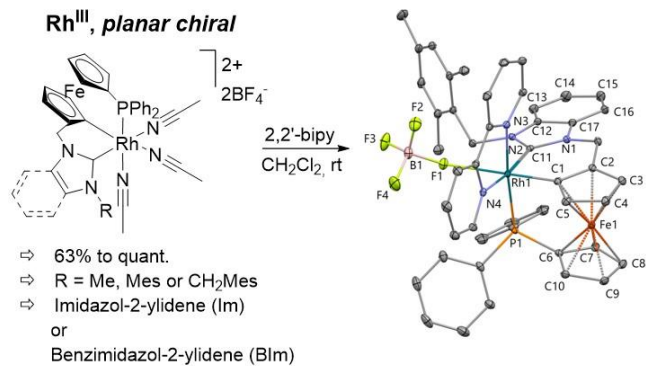
The authors thank the Centre National de la Recherche Scientifique (CNRS) for financial support.

REFERENCES

1. D. A. Colby, R. G. Bergman and J. A. Ellman, *Chem. Rev.*, 2010, **110**, 624-655.
2. D. A. Colby, A. S. Tsai, R. G. Bergman and J. A. Ellman, *Acc. Chem. Res.*, 2012, **45**, 814-825.
3. J. Wencel-Delord, T. Dröge, F. Liu and F. Glorius, *Chem. Soc. Rev.*, 2011, **40**, 4740-4761.
4. N. Kuhl, N. Schröder and F. Glorius, *Adv. Synth. Catal.*, 2014, **356**, 1443-1460.
5. G. Song, F. Wang and X. Li, *Chem. Soc. Rev.*, 2012, **41**, 3651-3678.
6. G. Song and X. Li, *Acc. Chem. Res.*, 2015, **48**, 1007-1020.
7. T. Gensch, M. J. James, T. Dalton and F. Glorius, *Angew. Chem. Int. Ed.*, 2018, **57**, 2296-2306.
8. S. Rej and N. Chatani, *Angew. Chem. Int. Ed.*, 2019, **58**, 8304-8329.
9. C. Wang, F. Chen, P. Qian and J. Cheng, *Org. Biomol. Chem.*, 2021, **19**, 1705-1721.
10. A. V. Kolos and D. S. Perekalin, *Mendeleev Commun.*, 2021, **31**, 1-7.
11. V. V. Grushin, W. J. Marshall and D. L. Thorn, *Adv. Synth. Catal.*, 2001, **343**, 161-165.
12. T. K. Hyster, L. Knörr, T. R. Ward and T. Rovis, *Science*, 2012, **338**, 500-503.
13. B. Ye and N. Cramer, *Science*, 2012, **338**, 504-506.
14. J. Zheng, W.-J. Cui, C. Zheng and S.-L. You, *J. Am. Chem. Soc.*, 2016, **138**, 5242-5245.

15. Z.-J. Jia, C. Merten, R. Gontla, C. G. Daniliuc, A. P. Antonchick and H. Waldmann, *Angew. Chem. Int. Ed.*, 2017, **56**, 2429-2434.
16. E. A. Trifonova, N. M. Ankudinov, A. A. Mikhaylov, D. A. Chusov, Y. V. Nelyubina and D. S. Perekalin, *Angew. Chem. Int. Ed.*, 2018, **57**, 7714-7718.
17. J. Wencel-Delord and F. Colobert, *Chem.–Eur. J.*, 2013, **19**, 14010-14017.
18. S. Motevalli, Y. Sokeirik and A. Ghanem, *Eur. J. Org. Chem.*, 2016, **2016**, 1459-1475.
19. C. G. Newton and N. Cramer, in *Rhodium Catalysis in Organic Synthesis*, ed. K. Tanaka, Wiley-VCH Verlag GmbH & Co. KGaA, Weinheim, 2019, DOI: <https://doi.org/10.1002/9783527811908.ch21>, pp. 629-644.
20. T. Yoshino, S. Satake and S. Matsunaga, *Chem.–Eur. J.*, 2020, **26**, 7346-7357.
21. A. Labande, N. Debono, A. Sournia-Saquet, J.-C. Daran and R. Poli, *Dalton Trans.*, 2013, **42**, 6531-6537.
22. N. Debono, J.-C. Daran, R. Poli and A. Labande, *Polyhedron*, 2015, **86**, 57-63.
23. N. G. Connelly and W. E. Geiger, *Chem. Rev.*, 1996, **96**, 877-910.
24. S. Gülcemal, A. Labande, J.-C. Daran, B. Cetinkaya and R. Poli, *Eur. J. Inorg. Chem.*, 2009, **2009**, 1806-1815.
25. A. Labande, J.-C. Daran, E. Manoury and R. Poli, *Eur. J. Inorg. Chem.*, 2007, **2007**, 1205-1209.
26. E. Mas-Marzá, M. Poyatos, M. Sanaú and E. Peris, *Organometallics*, 2003, **23**, 323-325.
27. M. Poyatos, M. Sanaú and E. Peris, *Inorg. Chem.*, 2003, **42**, 2572-2576.
28. M. Feller, E. Ben-Ari, T. Gupta, L. J. W. Shimon, G. Leitus, Y. Diskin-Posner, L. Weiner and D. Milstein, *Inorg. Chem.*, 2007, **46**, 10479-10490.
29. B. Rybtchinski, S. Oevers, M. Montag, A. Vigalok, H. Rozenberg, J. M. L. Martin and D. Milstein, *J. Am. Chem. Soc.*, 2001, **123**, 9064-9077.
30. H. Salem, Y. Ben-David, L. J. W. Shimon and D. Milstein, *Organometallics*, 2006, **25**, 2292-2300.
31. H. Salem, G. Leitus, L. J. W. Shimon, Y. Diskin-Posner and D. Milstein, *Inorg. Chim. Acta*, 2011, **369**, 260-269.
32. S. Wei, J. Pedroni, A. Meißner, A. Lumbroso, H.-J. Drexler, D. Heller and B. Breit, *Chem.–Eur. J.*, 2013, **19**, 12067-12076.
33. L. Yang, C. A. Correia and C.-J. Li, *Adv. Synth. Catal.*, 2011, **353**, 1269-1273.
34. V. M. Chernyshev, E. A. Denisova, D. B. Eremin and V. P. Ananikov, *Chem. Sci.*, 2020, **11**, 6957-6977.
35. no COD hydrogenation was observed for **1a** under 3 bar H₂ in THF for 16h.
36. N. Guimond, S. I. Gorelsky and K. Fagnou, *J. Am. Chem. Soc.*, 2011, **133**, 6449-6457.

Graphical Abstract:



Supplementary Information for :

Oxidation-Promoted Synthesis of Ferrocenyl Planar Chiral Rhodium(III) Complexes for C-H Functionalization Catalysis

Julien Cabanes,[†] Maskym Odnoroh,[†] Carine Duhayon,[†] Christian Bijani,[†] Alix Sournia-Saquet,[†] Rinaldo Poli^{†,‡} and Agnès Labande^{*,†}.

[†] LCC-CNRS, Université de Toulouse, CNRS, INPT, F-31077 Toulouse, France; e-mail: agnes.labande@lcc-toulouse.fr

[‡] Institut Universitaire de France, 1 rue Descartes, 75231 Paris, France.

General Considerations	p. 1
1- Synthetic procedures for all new compounds	p. 2
2- Cyclic voltammograms of complexes 1b and 1c	p. 4
3- NMR spectra of complexes 3a-c and of the products obtained from the reactions of 3b and 3c with bipy	p. 5
4- X-Ray structural analyses: Mercury representations of complexes 4a and 5c X-ray data collection and structure determination of complex 5c .	p. 10

GENERAL CONSIDERATIONS

All manipulations were performed under an inert atmosphere of dry argon by using vacuum line and Schlenk tube techniques. Solvents for syntheses were dried and degassed by standard methods before use. Commercial chemicals were from Acros, Aldrich, Alfa Aesar, or Fluka and used as received. The rhodium(I) complexes **1a-c** were prepared according to previously reported procedures.^{1,2}

1D- and 2D-NMR spectra were recorded on Bruker AvanceIII 400 and Avance NEO 600 spectrometers. Chemical shifts (δ) for all nuclei are given in ppm. For ¹H and ¹³C, the residual peak of deuterated solvents was used as reference. External reference for ³¹P is 85% H₃PO₄. Peaks are labeled as singlet (s), doublet (d), triplet (t), multiplet (m) and broad (br). The proton and carbon assignments were performed by COSY, HSQC, ¹H-¹³C HMBC experiments.

Electrospray (ES) mass spectra were recorded at the Université Paul Sabatier by the Service Commun de Spectrométrie de Masse on a MS/MS API-365 (Perkin Elmer Sciex).

Cyclic voltammetry (CV) experiments were carried out with an Autolab PGSTAT100 potentiostat (Metrohm). Experiments were performed at room temperature in a homemade airtight three-electrode cell connected to a vacuum/argon line. The reference electrode consisted of a saturated calomel electrode (SCE) separated from the solution by a bridge compartment. The counter electrode was a platinum wire of ca 1cm² apparent surface. The working electrode was a Pt microdisk (0.5 mm diameter). The supporting electrolyte [NBu₄][BF₄] (Fluka, 99% electrochemical grade) was dried and degassed under argon. CH₂Cl₂ was freshly distilled over CaH₂ prior to use. The solutions used during the electrochemical studies were typically 10⁻³ M in rhodium compound and 0,1 M in supporting electrolyte. Before each measurement, the solutions were degassed by bubbling Ar and the working electrode was polished with a polishing machine (Presi P230). All electrochemical data are referenced versus ferrocene (in our hands, E°[FcH/FcH⁺] = 0.54 V/SCE in CH₂Cl₂/n-Bu₄BF₄, 0.1 V.s⁻¹, 25°C).

X-ray structural analyses.

A single crystal suitable for X-ray diffraction was coated with paratone oil and mounted onto the goniometer. The X-ray crystallographic data were obtained at low temperature from a Bruker Apex2 diffractometer (MoK α radiation source) equipped with an Oxford Cryosystem. The structure has been solved with SUPERFLIP³ and refined by means of least-square procedures on F using the PC version of the program CRYSTALS.⁴ The scattering factors for all the atoms were used as listed in the International Tables for X-ray Crystallography. Absorption correction was performed using a multi-scan procedure. All non-hydrogen atoms were refined anisotropically. The H atoms were located in a difference map, but those attached to carbon atoms were repositioned geometrically. The H atoms were initially refined with soft restraints on the bond lengths and angles to regularize their geometry and U[iso](H) (in the range 1.2-1.5 times U[eq] of the parent atom), after which the positions were refined with riding constraints. The drawing of the molecules was realized with the help of Mercury. Crystal data and refinement parameters are shown pages 10-24.

1- SYNTHETIC PROCEDURES

[Rh(Fe(C₅H₄PPh₂)(C₅H₄CH₂Im^{Me}))(CH₃CN)₃]²⁺.2BF₄⁻ (3a).⁵ A solution of [N(4-BrC₆H₄)₃][BF₄] **2** (142 mg, 2.49 10⁻⁴ moles) in MeCN (8 mL + 3x4 mL for rinsing) was slowly added to a solution of [Rh(ImMe)(COD)]⁺.BF₄⁻ **1a** (100 mg, 1.31 10⁻⁴ moles) in MeCN (20 mL) at room temperature. The reaction mixture was heated at 50°C for 20h, during which the color changed from dark brown-green to bright orange and a white precipitate appeared. After cooling to room temperature, the mixture was concentrated to ca. 5 mL and an excess of MTBE was added. The orange-red precipitate was filtered on Celite®, washed with MTBE and recovered by addition of MeCN. The MeCN solution was concentrated and the orange-red solid was dried in vacuo (113 mg, quantitative yield). ¹H NMR (400 MHz, CD₃CN, 298 K) δ 7.66-7.60 (3H, m, PPh₂); 7.56-7.49 (3H, m, PPh₂); 7.46-7.41 (2H, m, PPh₂); 7.44 (1H, d, J=2.1Hz, CH=C Im); 7.24 (1H, d, J_{HH}=2.0Hz, CH=C Im), 7.18-7.12 (2H, m, PPh₂); 5.49 (1H, m, Cp); 4.91, 4.80 (2*1H, d, J_{HH}=16.3Hz, CH₂Im); 4.77 (1H, m, Cp); 4.70 (2H, dd, J_{HH}=2.4Hz, J_{HH}=1.2Hz, Cp); 4.59 (1H, dd, J_{HH}=2.5Hz, J_{HH}=1.2Hz, Cp); 4.37 (1H, m, Cp); 4.23 (1H, t, J_{HH}=2.4Hz, Cp); 3.87 (3H, s, CH₃Im). ³¹P NMR (161.99 MHz, CD₃CN, 298 K) δ 41.6 (d, J_{RhP}=139.4 Hz).

[Rh(Fe(C₅H₄PPh₂)(C₅H₄CH₂Im^{Mes}))(CH₃CN)₃]²⁺.2BF₄⁻ (3b). [N(4-BrC₆H₄)₃][BF₄] **2** (61.5 mg, 1.09 10⁻⁴ moles), MeCN (4 mL + 3x2 mL for rinsing), [Rh(ImMes)(COD)]⁺.BF₄⁻ **1b** (50 mg, 5.77 10⁻⁵ moles), MeCN (10 mL). Orange-red solid (44 mg, 79% yield). ¹H NMR (400 MHz, CD₃CN, 298 K) δ 7.68-7.64 (1H, m, PPh₂); 7.59 (1H, d, J_{HH}=2.0Hz, CH=C Im); 7.55-7.49 (6H, m, CH=C Im + PPh₂); 7.47-7.43 (2H, m, PPh₂), 7.15+7.12 (2H, s, CH Mes); 7.0-6.94 (2H, m, PPh₂); 5.74 (1H, dt, J_{HH}=2.5Hz, J_{HH}=1.2Hz, Cp^P); 5.16 (1H, d, J_{HH}=16.7Hz, CH₂Im); 5.06 (1H, d, J_{HH}=16.6Hz, CH₂Im); 4.80 (1H, dt, J_{HH}=2.6Hz, J_{HH}=1.2Hz, Cp^P); 4.72 (1H, dd, J_{HH}=2.3Hz, J_{HH}=1.2Hz, Cp^C); 4.69 (1H, dd, J_{HH}=2.4Hz, J_{HH}=1.2Hz, Cp^C); 4.65-4.62 (1H, m, Cp^P); 4.20 (1H, t, J_{HH}=2.4 Hz, Cp^C); 4.09 (1H, dt, J_{HH}=2.6Hz, J_{HH}=1.3Hz, Cp^P); 2.50 (3H, s, *o*-CH₃Mes); 2.38 (3H, s, *p*-CH₃Mes); 1.77 (3H, s, *o*-CH₃Mes). ¹³C NMR (100.63 MHz, CD₃CN, 298 K) δ 147.6 (dd, J_{RhC}=49.0Hz, J_{PC}=12.4Hz, quat C_{NHC}); 140.7 (quat *p*-C_{Mes}), 137.1 (quat *o*-C_{Mes}), 136.5 (quat *o*-C_{Mes}), 134.9 (quat C_{Mes}), 134.0 (J_{PC}=48.6Hz, quat C_{PPh2}), 133.2 (d, J_{PC}=2.8Hz, CH_{PPh2}), 132.9 (d, J_{PC}=10.7Hz, 2*CH_{PPh2}), 131.6 (d, J_{PC}=9.9Hz, 2*CH_{PPh2}), 131.3 (d, J_{PC}=3.1Hz, CH_{PPh2}), 129.4 (d, J_{PC}=10.8Hz, 2*CH_{PPh2}), 129.0+128.7 (2*CH_{Mes}), 128.5 (d, J_{PC}=10.9Hz, 2*CH_{PPh2}), 128.3 (quat C_{PPh2}, seen with ³¹P decoupling), 127.4+125.8 (2*CH_{Im}), 84.9 (d, J_{PC}=4.3Hz, quat C Cp^C_{Im}), 84.1 (d, J_{PC}=10.3Hz, CH Cp^P), 75.8 (d, J_{PC}=12.1Hz, CH Cp^P), 75.1 (CH Cp^C), 74.1 (d, J_{PC}=8.1Hz, CH Cp^P), 73.2 (d, J_{PC}=8.4Hz, CH Cp^P), 72.3 (CH Cp^C), 71.7 (d, J_{PC}=68.1Hz, quat C Cp^P), 70.4 (CH Cp^C), 66.6 (dd, J_{RhC}=29.6Hz, J_{PC}=5.6Hz, quat C Cp^C_{Rh}), 51.8 (CH₂Im), 20.0 (*p*-CH₃ Mes), 19.6+17.5 (2**o*-CH₃ Mes). ³¹P NMR (161.99 MHz, CD₃CN, 298 K) δ 41.2 (d, J_{RhP}=137.7 Hz). MS, ESI *m/z* 335 ([M-3xMeCN]²⁺, 100%). HRMS, ESI : calcd for C₃₅H₃₂FeN₂PRh 335.0354; found 335.0354.

[Rh(Fe(C₅H₄PPh₂)(C₅H₄CH₂BIm^{CH₂Mes}))(CH₃CN)₃]²⁺.2BF₄⁻ (3c). [N(4-BrC₆H₄)₃][BF₄] **2** (72.7 mg, 1.28 10⁻⁴ moles), MeCN (4 mL + 3x2 mL for rinsing), [Rh(BImCH₂Mes)(COD)]⁺.BF₄⁻ **1c** (51.9 mg, 6.81 10⁻⁵ moles),

MeCN (10 mL). Orange-red solid (36 mg, 63% yield). ^1H NMR (400 MHz, CD_3CN , 298 K) δ 7.77-7.71 (2H, m, PPh_2); 7.61-7.55 (3H, m, PPh_2); 7.53 (1H, m, CH BIm); 7.46-7.41 (2H, m, $\text{PPh}_2 + \text{CH BIm}$), 7.20 (1H, ddd, $J_{\text{HH}}=8.4\text{Hz}$, $J_{\text{HH}}=7.3\text{Hz}$, $J_{\text{HH}}=1.1\text{Hz}$, CH BIm); 7.13-7.09 (5H, m, $\text{PPh}_2 + \text{CH BIm}$); 6.80 (1H, br s, CH Mes); 6.66 (1H, d, $J_{\text{HH}}=8.5\text{Hz}$, CH BIm); 5.85 (1H, d, $J_{\text{HH}}=15.7\text{Hz}$, CH_2Mes); 5.45 (1H, m, Cp^{P}); 5.45 (1H, d, $J_{\text{HH}}=15.7\text{Hz}$, CH_2Mes); 5.38 (1H, d, $J_{\text{HH}}=16.5\text{Hz}$, CH_2Fc); 5.15 (1H, d, $J_{\text{HH}}=16.5\text{Hz}$, CH_2Fc); 4.92-4.91 (1H, m, Cp^{C}); 4.77-4.71 (3*1H, m, 2* $\text{Cp}^{\text{P}+}$ Cp^{C}); 4.40-4.39 (1H, m, Cp^{P}); 4.35 (1H, t, $J_{\text{HH}}=2.4\text{ Hz}$, Cp^{C}); 2.51 (3H, s, $o\text{-CH}_3\text{Mes}$); 2.30 (3H, s, $p\text{-CH}_3\text{Mes}$); 1.61 (3H, s, $o\text{-CH}_3\text{Mes}$). ^{13}C NMR (100.63 MHz, CD_3CN , 298 K) δ 161.4 (app. dd, $J_{\text{RhC}}=48.7\text{Hz}$, quat C_{NHC}); 138.6 (quat $p\text{-C}_{\text{Mes}}$), 137.5+137.2 (2*quat $o\text{-C}_{\text{Mes}}$), 134.8+134.5 (2*quat C_{BIm}), 132.7-132.4 (CH_{PPh_2}), 131.9 (d, $J_{\text{PC}}=48.3\text{Hz}$, quat C_{PPh_2}), 131.7 (d, $J_{\text{PC}}=6.8\text{Hz}$, CH_{PPh_2}), 130.2+129.7 (2* CH_{Mes}), 129.2 (d, $J_{\text{PC}}=50.7\text{Hz}$, quat C_{PPh_2}), 129.2 (d, $J_{\text{PC}}=10.9\text{Hz}$, CH_{PPh_2}), 128.7 (d, $J_{\text{PC}}=10.9\text{Hz}$, CH_{PPh_2}), 127.8 (quat C_{Mes}), 124.6 (2* CH_{BIm}), 112.5+111.2 (2* CH_{BIm}), 83.7 (d, $J_{\text{PC}}=3.0\text{Hz}$, quat $\text{C Cp}^{\text{C BIm}}$), 81.7 (d, $J_{\text{PC}}=10.2\text{Hz}$, CH Cp^{P}), 76.9 (d, $J_{\text{PC}}=12.3\text{Hz}$, CH Cp^{P}), 75.1 (CH Cp^{C}), 74.1 (d, $J_{\text{PC}}=8.0\text{Hz}$, CH Cp^{P}), 73.5 (d, $J_{\text{PC}}=8.4\text{Hz}$, CH Cp^{P}), 71.8+71.7 (2* CH Cp^{C}), 71.5 (d, $J_{\text{PC}}=69.3\text{Hz}$, quat C Cp^{P}), 65.8 (dd, $J_{\text{RhC}}=30.4\text{Hz}$, $J_{\text{PC}}=4.8\text{Hz}$, quat $\text{C Cp}^{\text{C Rh}}$), 49.9 (CH_2Mes), 47.6 (CH_2Fc), 20.8 ($o\text{-CH}_3\text{ Mes}$), 19.9 ($p\text{-CH}_3\text{ Mes}$), 18.6 ($o\text{-CH}_3\text{ Mes}$). ^{31}P NMR (161.99 MHz, CD_3CN , 298 K) δ 40.9 (d, $J_{\text{RhP}}=138.2\text{ Hz}$). MS, ESI m/z 367 ($[\text{M}-3\text{xMeCN}]^{2+}$, 100%), 735 ($[\text{M}+\text{H}-3\text{xMeCN}]^+$, 27%). HRMS, ESI : calcd for $\text{C}_{40}\text{H}_{36}\text{FeN}_2\text{PRh}$ 367.0511; found 367.0519.

Reaction of 3b and 3c with 2,2'-bipyridine. Complex **3b** (23.5 mg, $2.07 \cdot 10^{-5}$ mole) or **3c** (45.5 mg, $4.41 \cdot 10^{-5}$ mole) was dissolved in CH_2Cl_2 (10 mL) and 2,2'-bipyridine (5.7 mg, $3.7 \cdot 10^{-5}$ mole, with **3b**; 10.3 mg, $6.62 \cdot 10^{-5}$ mole, with **3c**) was added. The mixture was stirred at room temperature for 3 hours and the solvent was concentrated in vacuo to ca. 1 mL. A red solid was obtained by precipitation and washing with an excess of MTBE. X-Ray quality crystals of **5c** were obtained by slow diffusion of an MTBE layer on a solution of the red solid in acetone- d_6 .

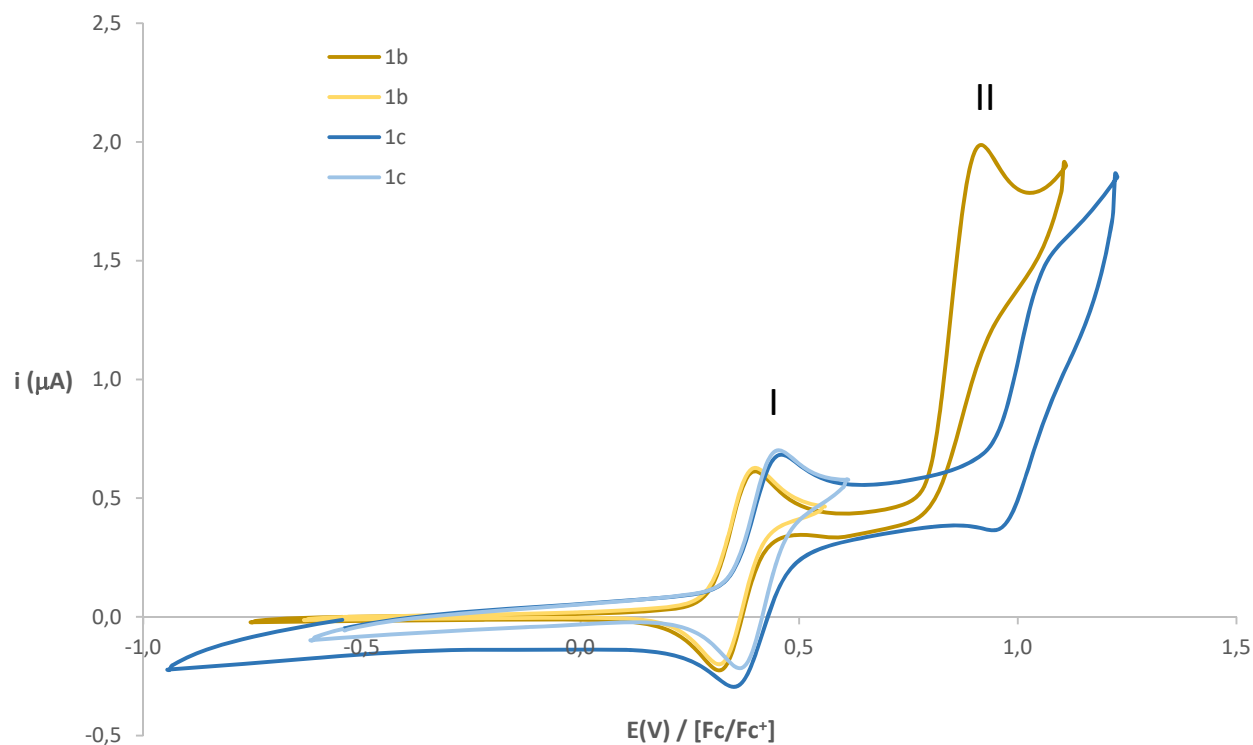
Arylation of 4-nitrobenzaldehyde (8) with 2-phenylpyridine (7). Typical procedure: 4-nitrobenzaldehyde (56.0 mg, $3.7 \cdot 10^{-4}$ mole) (**8**) and complex **3a** (8.0 mg, $9.3 \cdot 10^{-6}$ mole) were placed in a dry Schlenk tube and THF (0.5 mL) was added. 2-Phenylpyridine (26.5 μL , $1.9 \cdot 10^{-4}$ mole) (**7**) was added and the Schlenk tube was sealed and placed in a preheated bath. The mixture was stirred at 65°C for 24h, and the solvent was removed in vacuo. The residue was analyzed by ^1H NMR and the conversion into the desired alcohol (**9**) was determined by integration of characteristic signals: 2-phenylpyridine: δ 8.68 ppm, 1H, C(6)H; alcohol: 8.55 ppm, 1H, C(6)H or 5.58 ppm, 1H, CH(OH).

References

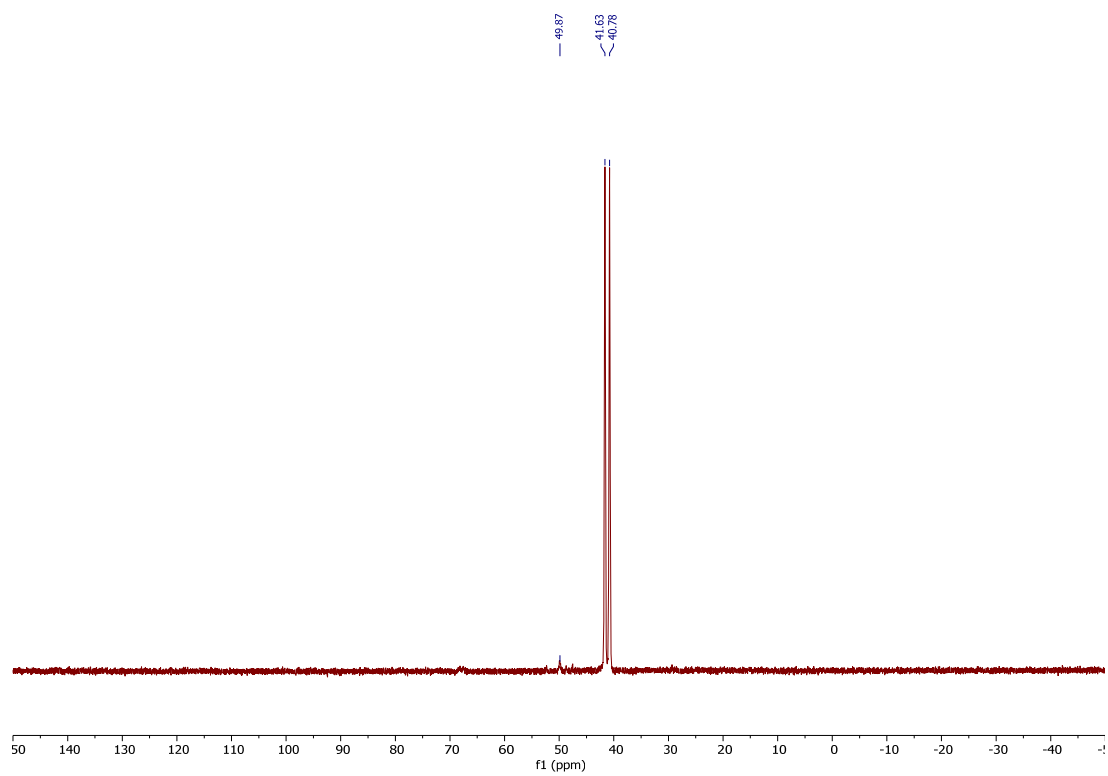
1. S. Gülcemal, A. Labande, J.-C. Daran, B. Cetinkaya and R. Poli, *Eur. J. Inorg. Chem.*, 2009, **2009**, 1806-1815.
2. A. Labande, J.-C. Daran, E. Manoury and R. Poli, *Eur. J. Inorg. Chem.*, 2007, **2007**, 1205-1209.
3. L. Palatinus and G. Chapuis, *J. Appl. Crystallogr.*, 2007, **40**, 786-790.
4. P. W. Betteridge, J. R. Carruthers, R. I. Cooper, K. Prout and D. J. Watkin, *J. Appl. Crystallogr.*, 2003, **36**, 1487.
5. A. Labande, N. Debono, A. Sournia-Saquet, J.-C. Daran and R. Poli, *Dalton Trans.*, 2013, **42**, 6531-6537.

2- CYCLIC VOLTAMMOGRAMS OF COMPLEXES **1B** AND **1C**

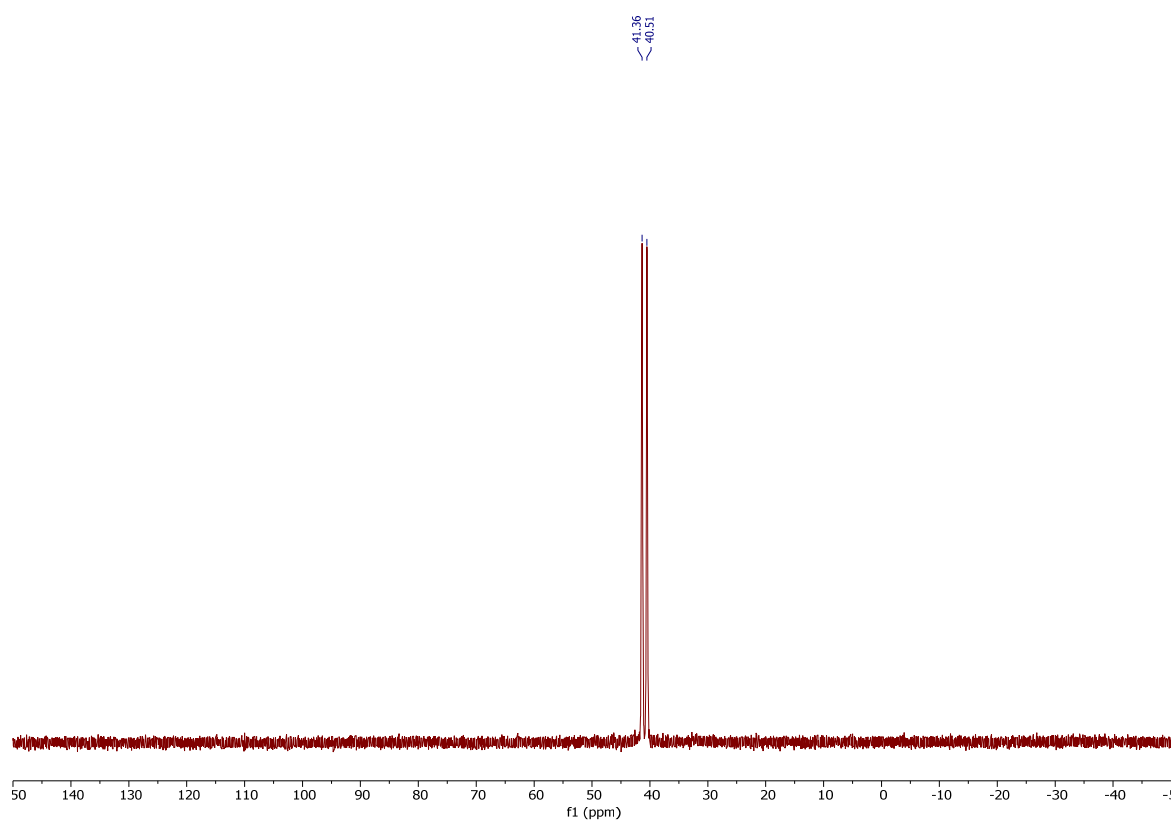
2.1. Cyclic voltammograms of complexes **1b** and **1c** on a Pt microelectrode, 1 mM in CH₂Cl₂ with [NBu₄][BF₄] (0.1M) at a scan rate of 0.1 V s⁻¹. Two potential limits were chosen (0.5 and 1.2 V vs [Fc/Fc⁺]). Peak I was attributed to the oxidation of the Fc moiety, Peak II can be ascribed to the oxidation of Rh.



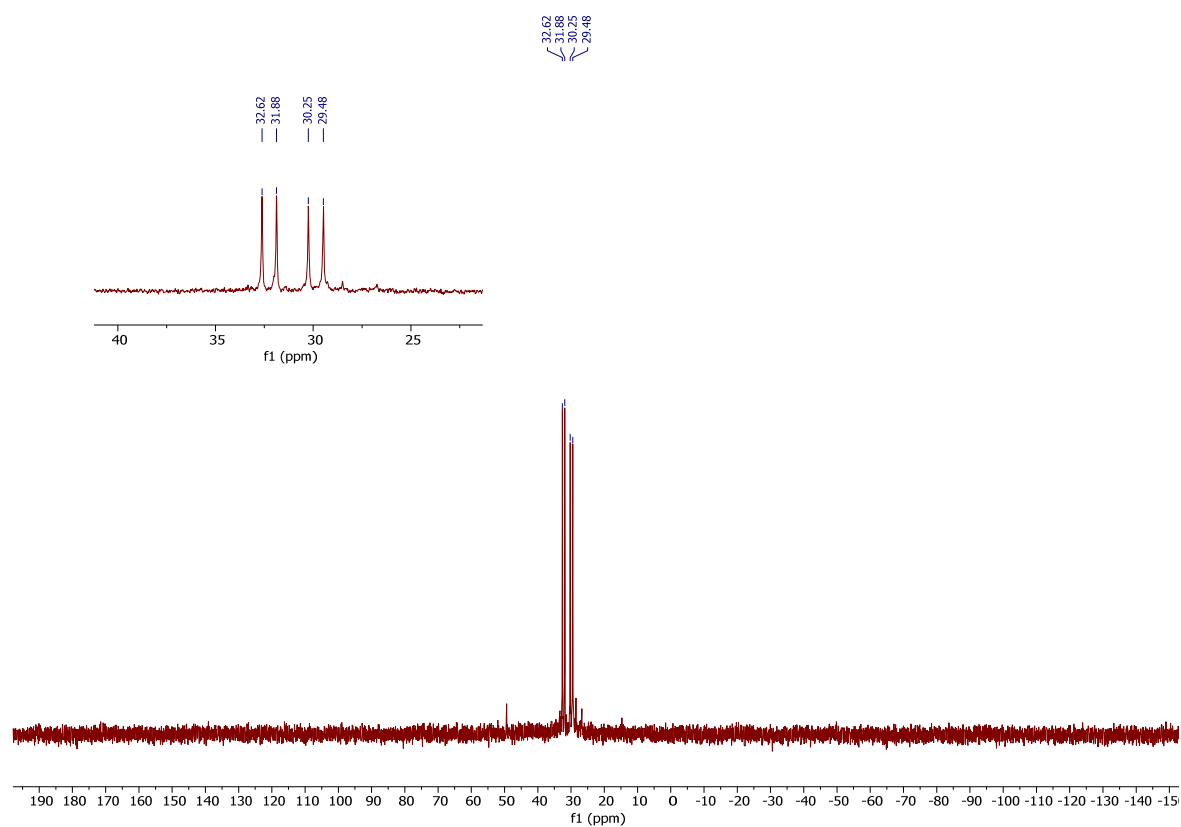
3.3. $^{31}\text{P}\{^1\text{H}\}$ spectrum of complex **3b** (161.99 MHz, CD_3CN , 298 K)



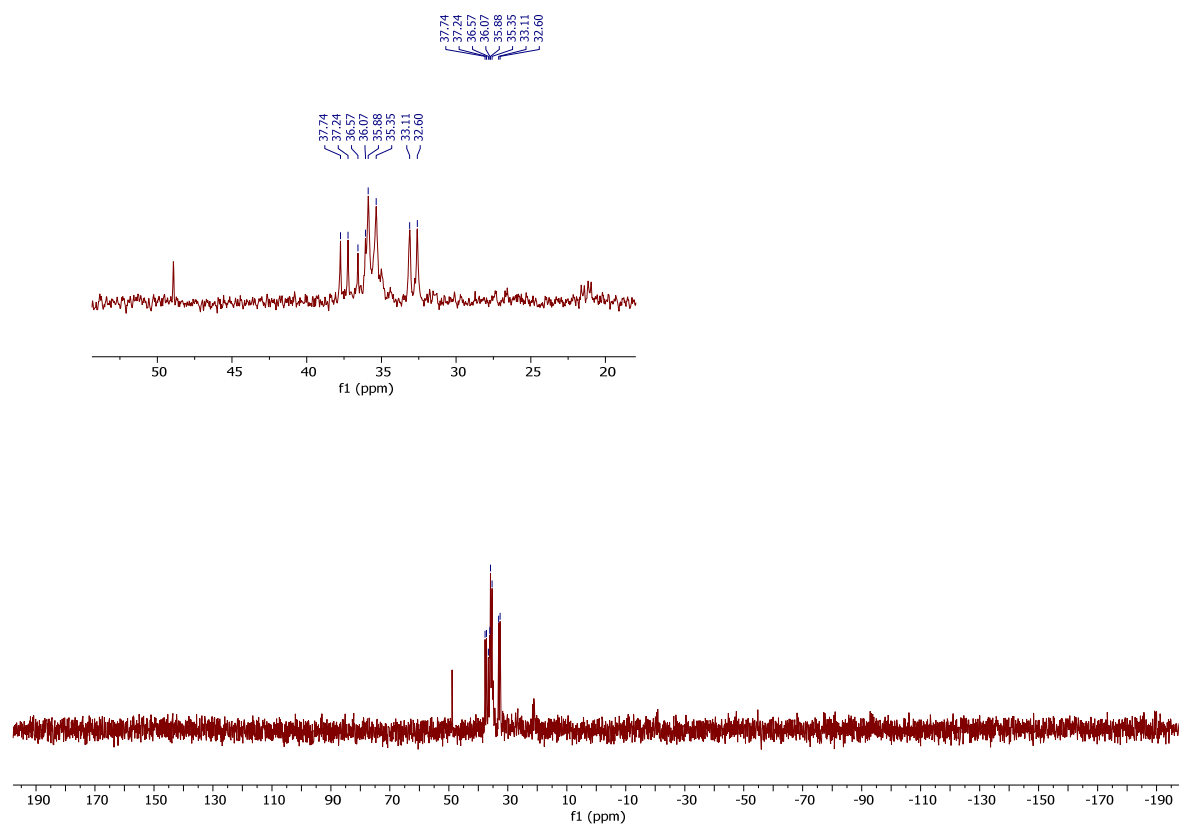
3.6. $^{31}\text{P}\{^1\text{H}\}$ NMR spectrum of **3c** (161.99 MHz, CD_3CN , 298 K)



3.7. $^{31}\text{P}\{^1\text{H}\}$ NMR spectrum of the product obtained from **3b** (161.99 MHz, acetone- d_6 , 298 K).

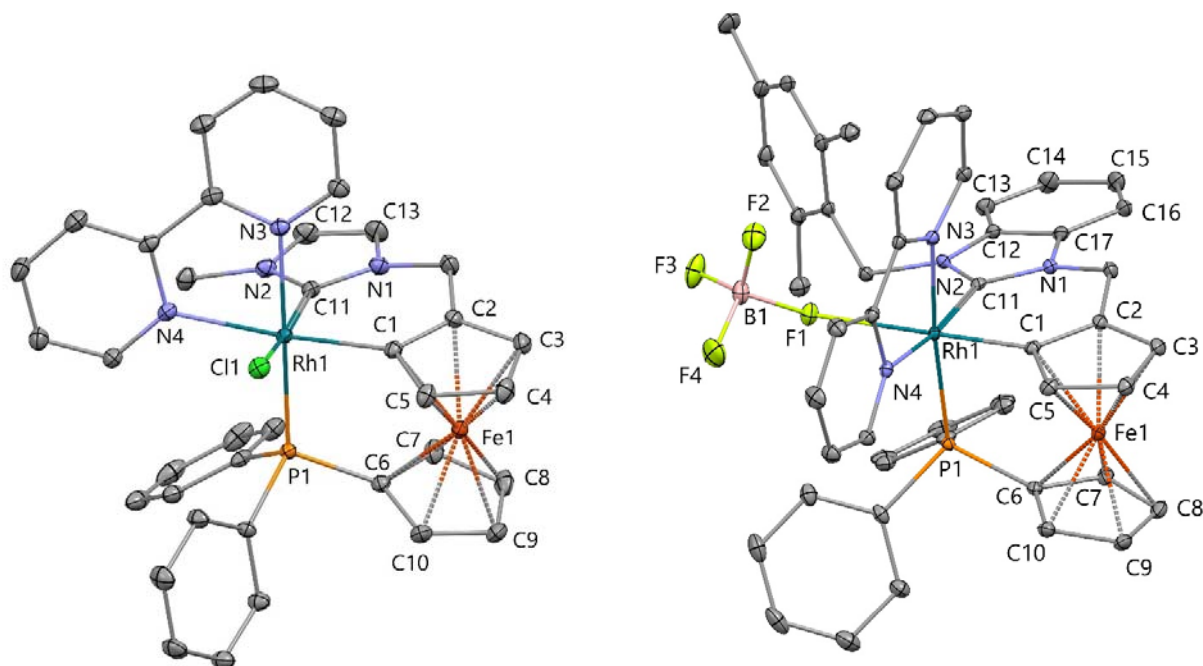


3.8. $^{31}\text{P}\{^1\text{H}\}$ NMR spectrum of the product obtained from **3c** (243.07 MHz, acetone- d_6 , 298 K).



4- X-RAY STRUCTURAL ANALYSES

4.1. Mercury representations of complexes **4a**⁵ (left) and **5c** (right). Ellipsoids are shown at the 50% (**4a**) or 30% (**5c**) probability level. All hydrogens are omitted for clarity.



4.2. Data collection and structure determination of complex **5c**

Crystal Data **5c**

a =	11.4449(8) Å	α =	97.060(2)°
b =	11.8714(8) Å	β =	94.539(2)°
c =	19.9736(15) Å	γ =	116.821(2)°

Volume	2375.54(18) Å ³	Crystal Class	triclinic
Space group	P -1	Z =	2
Formula	C ₅₃ H ₅₀ B ₂ F ₈ Fe ₁ N ₄ O ₁ P ₁ Rh ₁	Mr	1122.34
Cell determined from	9397 reflections	Cell θ range =	2 - 25°
Temperature	100K		
Shape	block		
Colour	dark red	Size	0.12 × 0.15 × 0.20 mm
D _x	1.57	F000	1144.000
μ	0.763 mm ⁻¹		
Absorption correction	multi-scan		
T _{min}	0.85	T _{max}	0.91

Data Collection

Diffractometer	multi-scan
Scan type	φ and ω scans
Reflections measured	93547
Independent reflections	8402
R _{int}	0.0322
θ_{\max}	25.0505
h =	-13 → 13
k =	-14 → 14
l =	-23 → 23

Refinement

$\Delta\rho_{\min}$ =	-0.39 e Å ⁻³
$\Delta\rho_{\max}$ =	0.49 e Å ⁻³
Reflections used	8141
Cutoff: I >	3.00 σ (I)
Parameters refined	640
S =	1.01
R-factor	0.021
weighted R-factor	0.026
Δ/σ_{\max}	0.0028
Refinement on	F
w =	$w' \times [1 - (\Delta F_{\text{obs}} / 6 \times \Delta F_{\text{est}})^2]^2$
w' =	$[P_0 T_0'(x) + P_1 T_1'(x) + \dots P_{n-1} T_{n-1}'(x)]^{-1}$, where P_i are the coefficients of a Chebychev series in $t_i(x)$, and $x = F_{\text{calc}}/F_{\text{calcmax}}$.
$P_0 - P_{n-1}$ =	0.688 0.441 0.449

Parameters

Label	<i>x</i>	<i>y</i>	<i>z</i>	U _{iso/equiv}	Occupancy
Rh1	.172117(8)	.216782(8)	.263894(4)	0.0100	1.0000
Fe1	.082577(16)	.035649(16)	.365663(8)	0.0130	1.0000
P1	0.11121(3)	0.06688(3)	.208816(15)	0.0113	1.0000
C1	0.14213(12)	0.16852(11)	0.35327(6)	0.0138	1.0000
C2	0.02092(13)	0.22611(12)	0.39924(6)	0.0153	1.0000
C3	0.03945(13)	0.15960(12)	0.45585(6)	0.0187	1.0000
C4	0.17342(13)	0.06249(13)	0.44589(6)	0.0189	1.0000
C5	0.23745(13)	0.06757(12)	0.38304(6)	0.0171	1.0000
C6	0.07175(12)	0.01907(11)	0.26876(6)	0.0140	1.0000
C7	0.05212(13)	0.01757(12)	0.31115(7)	0.0178	1.0000
C8	0.02699(14)	0.06306(13)	0.36101(7)	0.0215	1.0000
C9	0.11030(14)	0.14967(12)	0.35066(7)	0.0212	1.0000
C10	0.17197(13)	0.12374(12)	0.29403(6)	0.0181	1.0000
C11	0.02224(12)	0.34673(11)	0.27272(6)	0.0125	1.0000
C12	0.21957(12)	0.49297(11)	0.25039(6)	0.0152	1.0000
C13	0.32538(13)	0.57267(12)	0.22001(7)	0.0199	1.0000
C14	0.44931(13)	0.63095(13)	0.25972(8)	0.0264	1.0000
C15	0.46786(13)	0.61242(13)	0.32686(8)	0.0264	1.0000
C16	0.36363(13)	0.53130(12)	0.35642(7)	0.0204	1.0000
C17	0.23905(12)	0.47087(11)	0.31576(7)	0.0159	1.0000
C18	0.10101(13)	0.34579(12)	0.39615(6)	0.0175	1.0000
C19	0.02820(12)	0.40718(11)	0.15450(6)	0.0153	1.0000
C20	0.06911(12)	0.53550(11)	0.13110(6)	0.0148	1.0000
C21	0.03749(12)	0.62706(12)	0.16426(6)	0.0170	1.0000
C22	0.07905(13)	0.74440(12)	0.14202(7)	0.0204	1.0000
C23	0.15174(13)	0.77347(12)	0.08833(7)	0.0218	1.0000
C24	0.17733(13)	0.67979(13)	0.05449(7)	0.0203	1.0000
C25	0.13641(12)	0.56069(12)	0.07426(6)	0.0170	1.0000
C26	0.03845(14)	0.60392(13)	0.22364(7)	0.0226	1.0000
C27	0.20243(17)	0.90378(14)	0.06818(9)	0.0336	1.0000
C28	0.16803(14)	0.46493(13)	0.03369(7)	0.0227	1.0000

C29	0.23737(12)	0.06104(12)	0.14338(6)	0.0166	1.0000
C30	0.24853(14)	0.18430(13)	0.13338(7)	0.0212	1.0000
C31	0.34908(16)	0.28142(14)	0.08522(7)	0.0298	1.0000
C32	0.43692(14)	0.25544(15)	0.04626(7)	0.0312	1.0000
C33	0.42344(14)	0.13283(16)	0.05406(7)	0.0290	1.0000
C34	0.32430(13)	0.03532(14)	0.10266(7)	0.0224	1.0000
C35	0.03296(12)	0.13003(11)	0.16386(6)	0.0154	1.0000
C36	0.01585(14)	0.10866(12)	0.09257(7)	0.0192	1.0000
C37	0.12538(15)	0.15766(13)	0.05868(7)	0.0248	1.0000
C38	0.25200(15)	0.22592(13)	0.09524(8)	0.0269	1.0000
C39	0.27030(14)	0.24882(13)	0.16591(8)	0.0237	1.0000
C40	0.16105(13)	0.20224(12)	0.19999(7)	0.0181	1.0000
C41	0.13069(13)	0.46150(12)	0.35567(6)	0.0165	1.0000
C42	0.16788(13)	0.54113(12)	0.39438(6)	0.0193	1.0000
C43	0.30106(14)	0.50087(13)	0.39675(7)	0.0212	1.0000
C44	0.39261(13)	0.38122(13)	0.36078(7)	0.0193	1.0000
C45	0.34914(12)	0.30414(12)	0.32417(6)	0.0144	1.0000
C46	0.43873(12)	0.17088(12)	0.28988(6)	0.0149	1.0000
C47	0.57449(13)	0.11490(13)	0.28890(7)	0.0214	1.0000
C48	0.65246(13)	0.01157(14)	0.25822(7)	0.0245	1.0000
C49	0.59244(13)	0.08061(13)	0.23042(7)	0.0202	1.0000
C50	0.45656(12)	0.01985(12)	0.23362(6)	0.0157	1.0000
C51	-0.3776(2)	0.14688(18)	0.58620(11)	0.0483	1.0000
C52	0.25619(14)	0.25446(13)	0.57050(7)	0.0241	1.0000
C53	-0.2677(2)	0.2905(2)	0.50271(9)	0.0446	1.0000
N1	0.11623(10)	0.38046(10)	0.32794(5)	0.0138	1.0000
N2	0.08508(10)	0.41783(9)	0.22561(5)	0.0129	1.0000
N3	0.21922(10)	0.34549(10)	0.32074(5)	0.0134	1.0000
N4	0.37971(10)	0.10423(10)	0.26142(5)	0.0132	1.0000
O1	0.15681(14)	0.31090(15)	0.61104(8)	0.0588	1.0000
B1	0.36868(15)	0.28078(16)	0.13691(8)	0.0227	1.0000
B2	0.64151(15)	0.24566(15)	0.46858(8)	0.0220	1.0000
F1	0.26046(7)	0.26158(7)	0.16644(4)	0.0215	1.0000
F2	0.39910(10)	0.34916(10)	0.18653(5)	0.0379	1.0000

F3	0.32618(10)	0.34654(11)	0.08467(5)	0.0420	1.0000
F4	0.47370(9)	0.16116(10)	0.11368(6)	0.0450	1.0000
F5	0.62244(12)	0.13893(11)	0.46541(7)	0.0535	1.0000
F6	0.52625(9)	0.35636(10)	0.49371(5)	0.0417	1.0000
F7	0.68486(8)	0.25219(9)	0.40197(4)	0.0319	1.0000
F8	0.73736(9)	0.23727(8)	0.50973(4)	0.0300	1.0000
H31	0.03001(13)	0.17783(12)	0.49396(6)	0.0229	1.0000
H41	0.21276(13)	0.00151(13)	0.47659(6)	0.0236	1.0000
H51	0.32976(13)	0.00988(12)	0.36251(6)	0.0211	1.0000
H71	0.14021(13)	0.08788(12)	0.30797(7)	0.0207	1.0000
H81	0.09419(14)	0.05811(13)	0.39631(7)	0.0265	1.0000
H91	0.15734(14)	0.21441(12)	0.37861(7)	0.0253	1.0000
H101	0.26580(13)	0.16845(12)	0.27543(6)	0.0216	1.0000
H131	0.31324(13)	0.58703(12)	0.17440(7)	0.0244	1.0000
H141	0.52235(13)	0.68507(13)	0.24087(8)	0.0323	1.0000
H151	0.55234(13)	0.65564(13)	0.35280(8)	0.0311	1.0000
H161	0.37611(13)	0.51683(12)	0.40095(7)	0.0247	1.0000
H181	0.09922(13)	0.41847(12)	0.42600(6)	0.0210	1.0000
H182	0.17917(13)	0.33864(12)	0.41224(6)	0.0212	1.0000
H192	0.06789(12)	0.36177(11)	0.15111(6)	0.0203	1.0000
H191	0.05604(12)	0.35479(11)	0.12431(6)	0.0202	1.0000
H221	0.05694(13)	0.80725(12)	0.16392(7)	0.0246	1.0000
H241	0.22392(13)	0.69782(13)	0.01725(7)	0.0250	1.0000
H261	0.07548(14)	0.66343(13)	0.22924(7)	0.0362	1.0000
H262	0.01946(14)	0.61638(13)	0.26459(7)	0.0359	1.0000
H263	0.11089(14)	0.51655(13)	0.21544(7)	0.0357	1.0000
H271	0.21758(17)	0.89694(14)	0.02149(9)	0.0534	1.0000
H272	0.28536(17)	0.96109(14)	0.09477(9)	0.0533	1.0000
H273	0.13933(17)	0.93406(14)	0.07332(9)	0.0540	1.0000
H281	0.20937(14)	0.49945(13)	0.00432(7)	0.0347	1.0000
H282	0.22903(14)	0.44676(13)	0.06154(7)	0.0349	1.0000
H283	0.08953(14)	0.38607(13)	0.01607(7)	0.0345	1.0000
H301	0.18608(14)	0.20247(13)	0.15974(7)	0.0271	1.0000
H311	0.35637(16)	0.36642(14)	0.07898(7)	0.0360	1.0000

H321	0.50800(14)	0.32105(15)	0.01360(7)	0.0385	1.0000
H331	0.48420(14)	0.11582(16)	0.02641(7)	0.0352	1.0000
H341	0.31534(13)	0.04862(14)	0.10905(7)	0.0282	1.0000
H361	0.07011(14)	0.06142(12)	0.06728(7)	0.0233	1.0000
H371	0.11253(15)	0.14452(13)	0.01068(7)	0.0302	1.0000
H381	0.32625(15)	0.25586(13)	0.07153(8)	0.0316	1.0000
H391	0.35793(14)	0.29514(13)	0.19160(8)	0.0295	1.0000
H401	0.17350(13)	0.21961(12)	0.24818(7)	0.0221	1.0000
H411	0.03949(13)	0.48809(12)	0.35272(6)	0.0200	1.0000
H421	0.10116(13)	0.62202(12)	0.41952(6)	0.0245	1.0000
H431	0.33093(14)	0.55316(13)	0.42281(7)	0.0272	1.0000
H441	0.48446(13)	0.34996(13)	0.36209(7)	0.0245	1.0000
H471	0.61264(13)	0.16309(13)	0.30999(7)	0.0270	1.0000
H481	0.74518(13)	0.05047(14)	0.25683(7)	0.0307	1.0000
H491	0.64309(13)	0.16934(13)	0.20980(7)	0.0248	1.0000
H501	0.41368(12)	0.06690(12)	0.21492(6)	0.0198	1.0000
H512	-0.3678(2)	0.15384(18)	0.63490(11)	0.0765	1.0000
H511	-0.4542(2)	0.15390(18)	0.56826(11)	0.0766	1.0000
H513	-0.3803(2)	0.06745(18)	0.56482(11)	0.0763	1.0000
H532	-0.1802(2)	0.3423(2)	0.49313(9)	0.0683	1.0000
H531	-0.3202(2)	0.3351(2)	0.50321(9)	0.0678	1.0000
H533	-0.3118(2)	0.2117(2)	0.46907(9)	0.0683	1.0000

Thermal Parameters

Label	U ₁₁	U ₂₂	U ₃₃	U ₂₃	U ₁₃	U ₁₂
Rh1	0.00955(6)	0.01032(6)	0.01036(6)	0.00185(4)	0.00138(4)	0.00479(4)
Fe1	0.01429(9)	0.01273(9)	0.01218(9)	0.00319(7)	0.00120(7)	0.00642(7)
P1	0.01059(14)	0.01179(14)	0.01113(14)	0.00124(11)	0.00100(11)	0.00521(12)
C1	0.0170(6)	0.0138(6)	0.0135(6)	0.0026(4)	0.0041(5)	0.0094(5)
C2	0.0201(6)	0.0151(6)	0.0123(6)	0.0009(5)	0.0017(5)	0.0100(5)
C3	0.0252(7)	0.0198(6)	0.0122(6)	0.0013(5)	0.0016(5)	0.0118(5)
C4	0.0251(7)	0.0217(6)	0.0144(6)	0.0063(5)	0.0069(5)	0.0134(6)
C5	0.0177(6)	0.0195(6)	0.0179(6)	0.0050(5)	0.0065(5)	0.0109(5)
C6	0.0162(6)	0.0132(6)	0.0131(6)	0.0010(4)	0.0015(5)	0.0078(5)
C7	0.0171(6)	0.0214(6)	0.0176(6)	0.0020(5)	0.0021(5)	0.0116(5)

C8	0.0269(7)	0.0243(7)	0.0202(6)	0.0042(5)	0.0006(5)	0.0182(6)
C9	0.0306(7)	0.0150(6)	0.0206(6)	0.0049(5)	0.0028(5)	0.0125(6)
C10	0.0205(6)	0.0127(6)	0.0180(6)	0.0006(5)	0.0013(5)	0.0059(5)
C11	0.0145(6)	0.0108(5)	0.0139(6)	0.0009(4)	0.0016(4)	0.0078(5)
C12	0.0126(6)	0.0110(5)	0.0211(6)	0.0016(5)	-0.0007(5)	0.0055(5)
C13	0.0150(6)	0.0160(6)	0.0259(7)	0.0073(5)	0.0018(5)	0.0040(5)
C14	0.0134(6)	0.0204(6)	0.0390(8)	0.0113(6)	0.0015(6)	0.0012(5)
C15	0.0137(6)	0.0194(6)	0.0382(8)	0.0044(6)	-0.0077(6)	0.0029(5)
C16	0.0176(6)	0.0159(6)	0.0237(7)	0.0016(5)	-0.0054(5)	0.0064(5)
C17	0.0132(6)	0.0120(6)	0.0212(6)	0.0014(5)	0.0001(5)	0.0057(5)
C18	0.0196(6)	0.0167(6)	0.0126(6)	0.0009(5)	-0.0023(5)	0.0066(5)
C19	0.0161(6)	0.0128(6)	0.0134(6)	0.0022(5)	-0.0003(5)	0.0041(5)
C20	0.0118(6)	0.0135(6)	0.0161(6)	0.0036(5)	-0.0022(4)	0.0038(5)
C21	0.0141(6)	0.0168(6)	0.0174(6)	0.0019(5)	-0.0037(5)	0.0061(5)
C22	0.0191(6)	0.0154(6)	0.0242(7)	0.0002(5)	-0.0063(5)	0.0083(5)
C23	0.0189(6)	0.0157(6)	0.0257(7)	0.0070(5)	-0.0058(5)	0.0043(5)
C24	0.0158(6)	0.0207(6)	0.0210(6)	0.0099(5)	0.0001(5)	0.0045(5)
C25	0.0138(6)	0.0172(6)	0.0178(6)	0.0048(5)	-0.0007(5)	0.0053(5)
C26	0.0255(7)	0.0223(7)	0.0232(7)	0.0031(5)	0.0044(5)	0.0140(6)
C27	0.0382(9)	0.0215(7)	0.0394(9)	0.0149(6)	0.0000(7)	0.0111(6)
C28	0.0252(7)	0.0226(7)	0.0217(7)	0.0070(5)	0.0078(5)	0.0109(6)
C29	0.0121(6)	0.0202(6)	0.0132(6)	0.0004(5)	0.0022(4)	0.0042(5)
C30	0.0224(7)	0.0195(6)	0.0174(6)	0.0003(5)	0.0028(5)	0.0069(5)
C31	0.0322(8)	0.0218(7)	0.0235(7)	-0.0027(6)	0.0046(6)	0.0040(6)
C32	0.0206(7)	0.0362(8)	0.0177(7)	-0.0040(6)	0.0001(5)	-0.0004(6)
C33	0.0186(7)	0.0450(9)	0.0180(7)	0.0029(6)	-0.0012(5)	0.0115(6)
C34	0.0205(7)	0.0306(7)	0.0165(6)	0.0031(5)	0.0027(5)	0.0125(6)
C35	0.0175(6)	0.0123(6)	0.0201(6)	0.0043(5)	0.0078(5)	0.0090(5)
C36	0.0248(7)	0.0144(6)	0.0203(6)	0.0033(5)	0.0075(5)	0.0102(5)
C37	0.0391(8)	0.0170(6)	0.0233(7)	0.0057(5)	0.0174(6)	0.0150(6)
C38	0.0287(7)	0.0186(6)	0.0405(8)	0.0104(6)	0.0223(6)	0.0132(6)
C39	0.0181(6)	0.0173(6)	0.0384(8)	0.0065(6)	0.0093(6)	0.0094(5)
C40	0.0175(6)	0.0154(6)	0.0234(6)	0.0044(5)	0.0049(5)	0.0089(5)
C41	0.0189(6)	0.0140(6)	0.0164(6)	0.0042(5)	0.0018(5)	0.0074(5)

C42	0.0261(7)	0.0148(6)	0.0177(6)	0.0028(5)	0.0018(5)	0.0103(5)
C43	0.0305(7)	0.0198(6)	0.0195(6)	0.0021(5)	0.0059(5)	0.0170(6)
C44	0.0208(6)	0.0215(6)	0.0206(6)	0.0052(5)	0.0054(5)	0.0135(5)
C45	0.0171(6)	0.0173(6)	0.0116(5)	0.0047(5)	0.0018(4)	0.0099(5)
C46	0.0170(6)	0.0182(6)	0.0123(5)	0.0041(5)	0.0028(4)	0.0102(5)
C47	0.0175(6)	0.0256(7)	0.0222(7)	-0.0010(5)	0.0026(5)	0.0125(6)
C48	0.0127(6)	0.0287(7)	0.0287(7)	0.0006(6)	0.0030(5)	0.0079(6)
C49	0.0164(6)	0.0188(6)	0.0221(6)	0.0013(5)	0.0016(5)	0.0061(5)
C50	0.0164(6)	0.0162(6)	0.0152(6)	0.0029(5)	0.0031(5)	0.0080(5)
C51	0.0508(11)	0.0351(9)	0.0604(12)	0.0192(9)	0.0176(9)	0.0171(9)
C52	0.0271(7)	0.0203(6)	0.0243(7)	-0.0005(5)	-0.0011(6)	0.0125(6)
C53	0.0709(13)	0.0574(11)	0.0355(9)	0.0204(8)	0.0234(9)	0.0503(11)
N1	0.0135(5)	0.0123(5)	0.0146(5)	0.0015(4)	-0.0005(4)	0.0059(4)
N2	0.0104(5)	0.0107(5)	0.0157(5)	0.0022(4)	0.0000(4)	0.0037(4)
N3	0.0155(5)	0.0136(5)	0.0129(5)	0.0039(4)	0.0021(4)	0.0079(4)
N4	0.0133(5)	0.0168(5)	0.0112(5)	0.0042(4)	0.0025(4)	0.0079(4)
O1	0.0412(8)	0.0533(8)	0.0632(9)	-0.0154(7)	-0.0236(7)	0.0173(7)
B1	0.0177(7)	0.0308(8)	0.0199(7)	0.0082(6)	0.0016(6)	0.0108(6)
B2	0.0198(7)	0.0201(7)	0.0251(8)	0.0027(6)	0.0022(6)	0.0090(6)
F1	0.0165(4)	0.0258(4)	0.0222(4)	0.0105(3)	0.0037(3)	0.0084(3)
F2	0.0411(5)	0.0522(6)	0.0314(5)	0.0082(4)	0.0083(4)	0.0306(5)
F3	0.0422(5)	0.0660(7)	0.0335(5)	0.0311(5)	0.0144(4)	0.0319(5)
F4	0.0251(5)	0.0408(5)	0.0537(6)	0.0029(5)	-0.0126(4)	0.0066(4)
F5	0.0671(7)	0.0435(6)	0.0811(8)	0.0329(6)	0.0412(6)	0.0426(6)
F6	0.0285(5)	0.0435(5)	0.0279(5)	-0.0018(4)	-0.0024(4)	-0.0018(4)
F7	0.0225(4)	0.0504(5)	0.0223(4)	-0.0017(4)	0.0001(3)	0.0190(4)
F8	0.0306(5)	0.0321(5)	0.0289(4)	0.0044(4)	0.0107(4)	0.0152(4)

Distances

Rh1	P1	2.3711(3)Å		Rh1	C1	1.9912(12)Å
Rh1	C11	2.0330(12)Å		Rh1	N3	2.0805(10)Å
Rh1	N4	2.1291(10)Å		Rh1	F1	2.3500(7)Å
Fe1	C1	2.0132(12)Å		Fe1	C2	2.0427(12)Å
Fe1	C3	2.0509(12)Å		Fe1	C4	2.0463(12)Å
Fe1	C5	2.0192(12)Å		Fe1	C6	1.9962(12)Å

Fe1	C7	2.0285(13)Å		Fe1	C8	2.0668(13)Å
Fe1	C9	2.0551(13)Å		Fe1	C10	2.0075(12)Å
P1	C6	1.8191(12)Å		P1	C29	1.8259(12)Å
P1	C35	1.8370(12)Å		C1	C2	1.4224(18)Å
C1	C5	1.4415(17)Å		C2	C3	1.4329(18)Å
C2	C18	1.4886(18)Å		C3	C4	1.4212(19)Å
C3	H31	0.983Å		C4	C5	1.4247(18)Å
C4	H41	0.980Å		C5	H51	0.981Å
C6	C7	1.4418(17)Å		C6	C10	1.4401(17)Å
C7	C8	1.4220(19)Å		C7	H71	0.990Å
C8	C9	1.417(2)Å		C8	H81	0.977Å
C9	C10	1.4239(19)Å		C9	H91	0.986Å
C10	H101	0.973Å		C11	N1	1.3598(16)Å
C11	N2	1.3674(16)Å		C12	C13	1.3976(18)Å
C12	C17	1.3835(19)Å		C12	N2	1.3936(16)Å
C13	C14	1.3861(19)Å		C13	H131	0.958Å
C14	C15	1.400(2)Å		C14	H141	0.937Å
C15	C16	1.383(2)Å		C15	H151	0.935Å
C16	C17	1.3992(18)Å		C16	H161	0.938Å
C17	N1	1.3943(16)Å		C18	N1	1.4719(16)Å
C18	H181	0.996Å		C18	H182	0.970Å
C19	C20	1.5245(16)Å		C19	N2	1.4807(15)Å
C19	H192	0.974Å		C19	H191	0.984Å
C20	C21	1.4026(18)Å		C20	C25	1.4090(18)Å
C21	C22	1.3971(18)Å		C21	C26	1.5050(19)Å
C22	C23	1.391(2)Å		C22	H221	0.959Å
C23	C24	1.386(2)Å		C23	C27	1.5072(18)Å
C24	C25	1.3940(18)Å		C24	H241	0.939Å
C25	C28	1.5070(19)Å		C26	H261	0.974Å
C26	H262	0.962Å		C26	H263	0.975Å
C27	H271	0.962Å		C27	H272	0.946Å
C27	H273	0.948Å		C28	H281	0.963Å
C28	H282	0.973Å		C28	H283	0.958Å
C29	C30	1.3974(19)Å		C29	C34	1.3970(19)Å

C30	C31	1.391(2)Å		C30	H301	0.971Å
C31	C32	1.388(2)Å		C31	H311	0.966Å
C32	C33	1.380(2)Å		C32	H321	0.956Å
C33	C34	1.391(2)Å		C33	H331	0.961Å
C34	H341	0.946Å		C35	C36	1.3972(18)Å
C35	C40	1.3969(18)Å		C36	C37	1.3932(19)Å
C36	H361	0.944Å		C37	C38	1.385(2)Å
C37	H371	0.941Å		C38	C39	1.385(2)Å
C38	H381	0.951Å		C39	C40	1.3913(19)Å
C39	H391	0.961Å		C40	H401	0.945Å
C41	C42	1.3813(18)Å		C41	N3	1.3426(16)Å
C41	H411	0.954Å		C42	C43	1.383(2)Å
C42	H421	0.957Å		C43	C44	1.385(2)Å
C43	H431	0.956Å		C44	C45	1.3869(18)Å
C44	H441	0.948Å		C45	C46	1.4771(17)Å
C45	N3	1.3499(17)Å		C46	C47	1.3843(19)Å
C46	N4	1.3557(16)Å		C47	C48	1.380(2)Å
C47	H471	0.944Å		C48	C49	1.381(2)Å
C48	H481	0.944Å		C49	C50	1.3797(19)Å
C49	H491	0.959Å		C50	N4	1.3432(17)Å
C50	H501	0.958Å		C51	C52	1.492(2)Å
C51	H512	0.959Å		C51	H511	0.963Å
C51	H513	0.972Å		C52	C53	1.483(2)Å
C52	O1	1.1964(19)Å		C53	H532	0.960Å
C53	H531	0.963Å		C53	H533	0.973Å
B1	F1	1.4512(17)Å		B1	F2	1.3691(19)Å
B1	F3	1.3683(18)Å		B1	F4	1.3733(19)Å
B2	F5	1.3744(19)Å		B2	F6	1.3740(18)Å
B2	F7	1.4062(18)Å		B2	F8	1.3976(18)Å

Angles

P1	Rh1	C1	90.06(3)°		P1	Rh1	C11	85.92(3)°
C1	Rh1	C11	91.62(5)°		P1	Rh1	N3	174.70(3)°
C1	Rh1	N3	84.73(4)°		C11	Rh1	N3	93.26(4)°
P1	Rh1	N4	102.67(3)°		C1	Rh1	N4	88.90(4)°

C11	Rh1	N4	171.40(4)°		N3	Rh1	N4	78.23(4)°
P1	Rh1	F1	98.50(2)°		C1	Rh1	F1	165.42(4)°
C11	Rh1	F1	100.71(4)°		N3	Rh1	F1	86.80(3)°
N4	Rh1	F1	77.75(3)°		C1	Fe1	C2	41.05(5)°
C1	Fe1	C3	69.55(5)°		C2	Fe1	C3	40.98(5)°
C1	Fe1	C4	69.87(5)°		C2	Fe1	C4	68.75(5)°
C3	Fe1	C4	40.59(5)°		C1	Fe1	C5	41.89(5)°
C2	Fe1	C5	69.07(5)°		C3	Fe1	C5	68.87(5)°
C4	Fe1	C5	41.02(5)°		C1	Fe1	C6	99.51(5)°
C2	Fe1	C6	117.87(5)°		C3	Fe1	C6	156.95(5)°
C4	Fe1	C6	155.98(5)°		C5	Fe1	C6	117.08(5)°
C1	Fe1	C7	121.06(5)°		C2	Fe1	C7	108.76(5)°
C3	Fe1	C7	125.65(5)°		C4	Fe1	C7	161.58(5)°
C5	Fe1	C7	156.71(5)°		C1	Fe1	C8	160.85(5)°
C2	Fe1	C8	129.26(5)°		C3	Fe1	C8	114.28(5)°
C4	Fe1	C8	126.03(5)°		C5	Fe1	C8	157.07(5)°
C1	Fe1	C9	152.25(5)°		C2	Fe1	C9	166.20(5)°
C3	Fe1	C9	128.69(5)°		C4	Fe1	C9	109.11(5)°
C5	Fe1	C9	118.91(5)°		C1	Fe1	C10	114.32(5)°
C2	Fe1	C10	152.15(5)°		C3	Fe1	C10	160.73(5)°
C4	Fe1	C10	121.26(5)°		C5	Fe1	C10	100.86(5)°
C6	Fe1	C7	41.98(5)°		C6	Fe1	C8	69.63(5)°
C7	Fe1	C8	40.62(5)°		C6	Fe1	C9	69.94(5)°
C7	Fe1	C9	68.68(5)°		C8	Fe1	C9	40.21(6)°
C6	Fe1	C10	42.16(5)°		C7	Fe1	C10	69.90(5)°
C8	Fe1	C10	68.75(5)°		C9	Fe1	C10	41.01(5)°
Rh1	P1	C6	111.69(4)°		Rh1	P1	C29	116.14(4)°
C6	P1	C29	103.57(6)°		Rh1	P1	C35	117.20(4)°
C6	P1	C35	104.47(6)°		C29	P1	C35	102.17(6)°
Rh1	C1	Fe1	124.33(6)°		Rh1	C1	C2	126.13(9)°
Fe1	C1	C2	70.58(7)°		Rh1	C1	C5	126.81(9)°
Fe1	C1	C5	69.28(7)°		C2	C1	C5	107.04(11)°
Fe1	C2	C1	68.36(7)°		Fe1	C2	C3	69.82(7)°
C1	C2	C3	108.57(11)°		Fe1	C2	C18	133.92(9)°

C1	C2	C18	127.23(11)°		C3	C2	C18	123.71(11)°
Fe1	C3	C2	69.20(7)°		Fe1	C3	C4	69.53(7)°
C2	C3	C4	107.99(11)°		Fe1	C3	H31	125.725°
C2	C3	H31	125.122°		C4	C3	H31	126.877°
Fe1	C4	C3	69.88(7)°		Fe1	C4	C5	68.47(7)°
C3	C4	C5	107.95(11)°		Fe1	C4	H41	125.713°
C3	C4	H41	125.261°		C5	C4	H41	126.757°
Fe1	C5	C1	68.83(7)°		Fe1	C5	C4	70.51(7)°
C1	C5	C4	108.42(11)°		Fe1	C5	H51	124.547°
C1	C5	H51	125.684°		C4	C5	H51	125.850°
Fe1	C6	P1	114.38(6)°		Fe1	C6	C7	70.21(7)°
P1	C6	C7	129.03(9)°		Fe1	C6	C10	69.34(7)°
P1	C6	C10	122.72(9)°		C7	C6	C10	106.70(11)°
Fe1	C7	C6	67.81(7)°		Fe1	C7	C8	71.14(7)°
C6	C7	C8	108.24(11)°		Fe1	C7	H71	125.476°
C6	C7	H71	127.177°		C8	C7	H71	124.561°
Fe1	C8	C7	68.24(7)°		Fe1	C8	C9	69.45(7)°
C7	C8	C9	108.48(11)°		Fe1	C8	H81	127.921°
C7	C8	H81	124.923°		C9	C8	H81	126.594°
Fe1	C9	C8	70.34(7)°		Fe1	C9	C10	67.70(7)°
C8	C9	C10	108.20(11)°		Fe1	C9	H91	125.407°
C8	C9	H91	126.847°		C10	C9	H91	124.898°
Fe1	C10	C6	68.50(7)°		Fe1	C10	C9	71.29(7)°
C6	C10	C9	108.38(11)°		Fe1	C10	H101	125.743°
C6	C10	H101	125.426°		C9	C10	H101	126.194°
Rh1	C11	N1	126.07(9)°		Rh1	C11	N2	127.80(9)°
N1	C11	N2	106.13(10)°		C13	C12	C17	121.42(11)°
C13	C12	N2	131.82(12)°		C17	C12	N2	106.67(11)°
C12	C13	C14	116.32(12)°		C12	C13	H131	122.092°
C14	C13	H131	121.590°		C13	C14	C15	122.07(13)°
C13	C14	H141	118.437°		C15	C14	H141	119.485°
C14	C15	C16	121.62(12)°		C14	C15	H151	119.877°
C16	C15	H151	118.505°		C15	C16	C17	116.12(12)°
C15	C16	H161	121.845°		C17	C16	H161	122.024°

C12	C17	C16	122.36(12)°		C12	C17	N1	106.52(10)°
C16	C17	N1	131.10(12)°		C2	C18	N1	115.22(10)°
C2	C18	H181	108.355°		N1	C18	H181	106.681°
C2	C18	H182	110.269°		N1	C18	H182	106.897°
H181	C18	H182	109.258°		C20	C19	N2	114.27(10)°
C20	C19	H192	109.312°		N2	C19	H192	107.627°
C20	C19	H191	109.176°		N2	C19	H191	107.976°
H192	C19	H191	108.316°		C19	C20	C21	120.85(11)°
C19	C20	C25	119.39(11)°		C21	C20	C25	119.74(11)°
C20	C21	C22	119.00(12)°		C20	C21	C26	122.25(11)°
C22	C21	C26	118.74(12)°		C21	C22	C23	121.95(12)°
C21	C22	H221	119.708°		C23	C22	H221	118.345°
C22	C23	C24	118.11(12)°		C22	C23	C27	120.81(13)°
C24	C23	C27	121.07(13)°		C23	C24	C25	121.96(12)°
C23	C24	H241	118.544°		C25	C24	H241	119.495°
C20	C25	C24	119.10(12)°		C20	C25	C28	123.05(11)°
C24	C25	C28	117.85(12)°		C21	C26	H261	109.085°
C21	C26	H262	109.927°		H261	C26	H262	109.915°
C21	C26	H263	110.495°		H261	C26	H263	108.624°
H262	C26	H263	108.776°		C23	C27	H271	109.003°
C23	C27	H272	109.996°		H271	C27	H272	106.487°
C23	C27	H273	109.482°		H271	C27	H273	110.343°
H272	C27	H273	111.467°		C25	C28	H281	109.450°
C25	C28	H282	110.993°		H281	C28	H282	108.064°
C25	C28	H283	111.390°		H281	C28	H283	108.066°
H282	C28	H283	108.773°		P1	C29	C30	121.11(10)°
P1	C29	C34	119.46(10)°		C30	C29	C34	119.43(12)°
C29	C30	C31	119.97(13)°		C29	C30	H301	120.312°
C31	C30	H301	119.714°		C30	C31	C32	120.03(14)°
C30	C31	H311	119.310°		C32	C31	H311	120.661°
C31	C32	C33	120.31(13)°		C31	C32	H321	121.517°
C33	C32	H321	118.174°		C32	C33	C34	120.14(14)°
C32	C33	H331	119.534°		C34	C33	H331	120.309°
C29	C34	C33	120.05(14)°		C29	C34	H341	119.137°

C33	C34	H341	120.810°		P1	C35	C36	120.32(10)°
P1	C35	C40	120.89(10)°		C36	C35	C40	118.78(12)°
C35	C36	C37	120.13(13)°		C35	C36	H361	119.991°
C37	C36	H361	119.880°		C36	C37	C38	120.38(13)°
C36	C37	H371	119.397°		C38	C37	H371	120.226°
C37	C38	C39	120.09(12)°		C37	C38	H381	119.620°
C39	C38	H381	120.287°		C38	C39	C40	119.74(13)°
C38	C39	H391	120.528°		C40	C39	H391	119.724°
C35	C40	C39	120.86(13)°		C35	C40	H401	119.473°
C39	C40	H401	119.672°		C42	C41	N3	122.33(12)°
C42	C41	H411	120.312°		N3	C41	H411	117.357°
C41	C42	C43	119.01(12)°		C41	C42	H421	119.459°
C43	C42	H421	121.521°		C42	C43	C44	118.78(12)°
C42	C43	H431	121.626°		C44	C43	H431	119.597°
C43	C44	C45	119.61(12)°		C43	C44	H441	120.931°
C45	C44	H441	119.419°		C44	C45	C46	123.09(11)°
C44	C45	N3	121.19(11)°		C46	C45	N3	115.64(11)°
C45	C46	C47	122.41(11)°		C45	C46	N4	116.00(11)°
C47	C46	N4	121.55(11)°		C46	C47	C48	119.67(12)°
C46	C47	H471	119.685°		C48	C47	H471	120.630°
C47	C48	C49	118.96(12)°		C47	C48	H481	120.418°
C49	C48	H481	120.615°		C48	C49	C50	118.64(12)°
C48	C49	H491	121.359°		C50	C49	H491	119.993°
C49	C50	N4	123.11(11)°		C49	C50	H501	119.443°
N4	C50	H501	117.441°		C52	C51	H512	106.812°
C52	C51	H511	109.062°		H512	C51	H511	112.056°
C52	C51	H513	107.146°		H512	C51	H513	110.374°
H511	C51	H513	111.164°		C51	C52	C53	116.01(15)°
C51	C52	O1	121.95(16)°		C53	C52	O1	122.01(17)°
C52	C53	H532	108.471°		C52	C53	H531	108.920°
H532	C53	H531	112.136°		C52	C53	H533	107.642°
H532	C53	H533	109.684°		H531	C53	H533	109.868°
C11	N1	C17	110.48(10)°		C11	N1	C18	129.37(10)°
C17	N1	C18	119.79(10)°		C11	N2	C12	110.16(10)°

C11	N2	C19	126.91(10)°		C12	N2	C19	122.42(10)°
Rh1	N3	C41	125.00(8)°		Rh1	N3	C45	115.91(8)°
C41	N3	C45	119.03(11)°		Rh1	N4	C46	113.76(8)°
Rh1	N4	C50	128.18(8)°		C46	N4	C50	118.01(10)°
F1	B1	F2	108.58(11)°		F1	B1	F3	107.08(11)°
F2	B1	F3	111.39(13)°		F1	B1	F4	106.83(12)°
F2	B1	F4	111.08(13)°		F3	B1	F4	111.64(13)°
F5	B2	F6	111.69(13)°		F5	B2	F7	108.08(13)°
F6	B2	F7	108.21(12)°		F5	B2	F8	110.57(12)°
F6	B2	F8	108.98(12)°		F7	B2	F8	109.26(11)°
Rh1	F1	B1	144.54(8)°					